

Correlation between South China and India and development of double rift systems in the South China–India Duo during late Neoproterozoic time

Bingbing Liu^{1,2,3}, Touping Peng^{1,2,†}, Weiming Fan^{3,4}, Guochun Zhao⁵, Jianfeng Gao⁶, Xiaohan Dong^{1,2,3}, Shili Peng^{1,2,3}, Limin Wu^{1,2,3}, and Bingxia Peng¹

¹State Key Laboratory of Isotope Geochemistry, Guangzhou Institute of Geochemistry, Chinese Academy of Sciences, Guangzhou 510640, China

²Chinese Academy of Sciences Center for Excellence in Deep Earth Science, Guangzhou 510640, China

³University of Chinese Academy of Sciences, Beijing 100049, China

⁴Chinese Academy of Sciences Center for Excellence in Tibetan Plateau Earth Sciences, Beijing 100101, China

⁵Department of Earth Sciences, The University of Hong Kong, Pokfulam Road, Hong Kong, China

⁶State Key Laboratory of Ore Deposit Geochemistry, Institute of Geochemistry, Chinese Academy of Sciences, Guiyang 550081, China

ABSTRACT

South China, India, and their derivative blocks preserve many similar magmatic and sedimentary records related to the tectonic transition from Rodinia to Gondwana. They provide crucial insights into not only the paleogeographic correlation between them but also the geodynamic mechanism for such a transition. Our new results, combined with published data from these blocks, reveal that South China remained linked with India at least from ca. 830 Ma to ca. 510 Ma and formed the South China–India Duo, which is located at the western margin of Rodinia. The identical magmatism and sedimentation reflect that double late Neoproterozoic rift systems in the South China–India Duo developed owing to the rollback of subducting oceanic slab beneath them. For example, an intracontinental rift developed along the Jiangnan–Aravalli–Delhi fold belt, which separated the Yangtze–Marwar block from the Cathaysia–Bundelkhand block. Another intra-arc rift developed contemporaneously along the northern and western margins of the Yangtze block, through the Marwar terrane of western India, and then into the Seychelles and Madagascar terranes. Such an intra-arc rift is the most feasible explanation for the common development of coeval arc-like and extension-related magmatic rocks and extensional sedimentary sequences on the western margin of the South China–India


Duo, in Seychelles and Madagascar, and even at other subduction zones. South China was finally separated from Indian Gondwana at ca. 510 Ma due to the opening of the Proto-Tethys Ocean.

INTRODUCTION

Supercontinents form when nearly all continental blocks on Earth collide with one another and assemble into a large, single landmass (Zhao et al., 2018a). Rodinia and Gondwana are the most important supercontinents in Earth's history (Zhao et al., 2018a). Increasing lines of evidence including reliable geological, paleomagnetic, and paleontological data have established that they formed at ca. 1.10 Ga and ca. 0.53 Ga ago, respectively (e.g., Cawood et al., 2013, 2018). Although the paleogeographic positions of major continental blocks in Rodinia and Gondwana have been widely accepted (Cawood et al., 2018; Zhao et al., 2018a), the tectonic evolution of some microcontinents in Rodinia and Gondwana during the transition from Rodinia to Gondwana remain poorly understood. In particular, South China and India, two important continental blocks in Asia, are documented to have been involved in the tectonic evolution of both Rodinia and Gondwana based on magmatic, sedimentary, and paleontological evidence (e.g., Jiang et al., 2003; Yang et al., 2004; Cawood et al., 2013, 2018; Metcalfe, 2013; Zhao et al., 2018b). Their paleogeographic positions, correlation in Rodinia and Gondwana, and their tectonic affinity are still the subject of debate (Jiang et al., 2003; Yang et al., 2004; Cawood et al., 2013, 2018; Metcalfe, 2013; Yao et al., 2014; Wang et al., 2017a, 2021; Zhao et al.,

2018b; Chen et al., 2021). Additionally, the tectonic framework and geodynamic mechanism for the tectonic evolution of supercontinents particularly during the transition from Rodinia to Gondwana remain unresolved (Li et al., 2002; Wang et al., 2017a; Cawood et al., 2018; Zhao et al., 2018b). Fortunately, in recent years, significant new data about Neoproterozoic–Early Paleozoic magmatic rocks and sedimentary sequences related to the tectonic evolution of these two landmasses in South China and India and even their derivative terranes/blocks have been published (Yao et al., 2014; Wang et al., 2017a, 2021; Zhao et al., 2018b; Chen et al., 2021). Combination of these data with other data sets and further analysis is crucial for decoding the aforementioned issues.

In this contribution, we present new U–Pb and Lu–Hf isotopic analyses of detrital zircons of the late Neoproterozoic and Ordovician sedimentary sequences from the Eastern Yidun subterrane of South China and combine them with other published data from South China and other Gondwana- and Rodinia-derived continents to re-evaluate the correlation between South China and India and decode their tectonic evolution during the transition from Rodinia to Gondwana. A new reconstruction model is suggested, which shows that South China was connected to India and formed the South China–India Duo during late Neoproterozoic–Early Cambrian time. The breakup time of South China from Indian Gondwana after the Early Cambrian due to the opening of the Proto-Tethys Ocean is further constrained. Also, we propose the development of double late Neoproterozoic rift systems in the South China–India Duo, including an intra-arc rift along its western margin and an intracontinental rift along

Touping Peng  <https://orcid.org/0000-0001-5740-7248>

[†]Corresponding author: tpeng08@126.com.

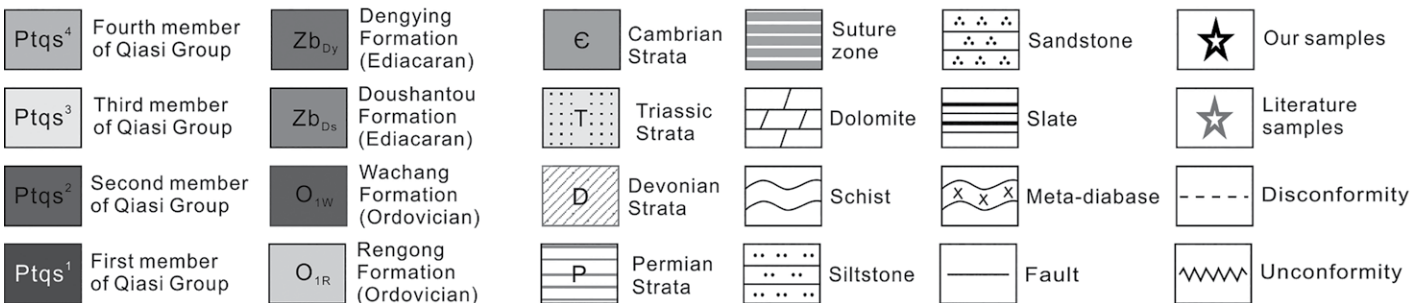
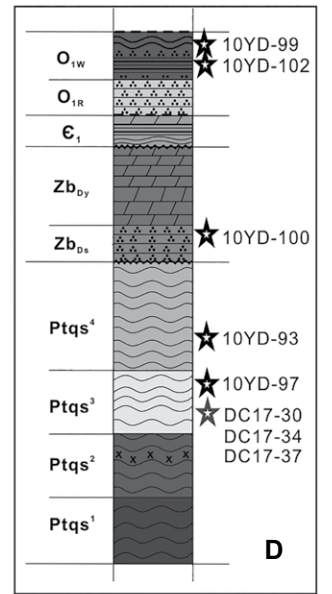
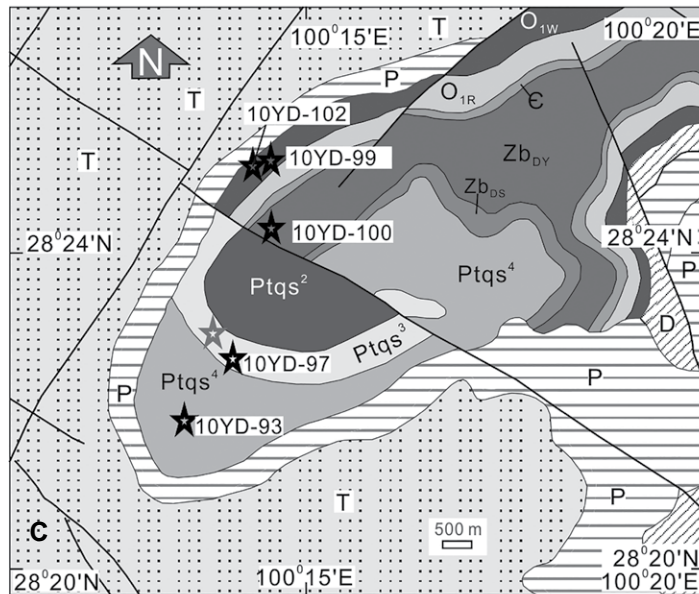
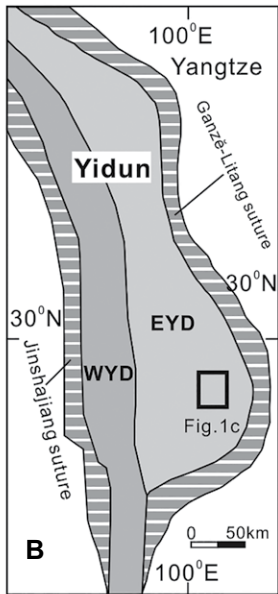
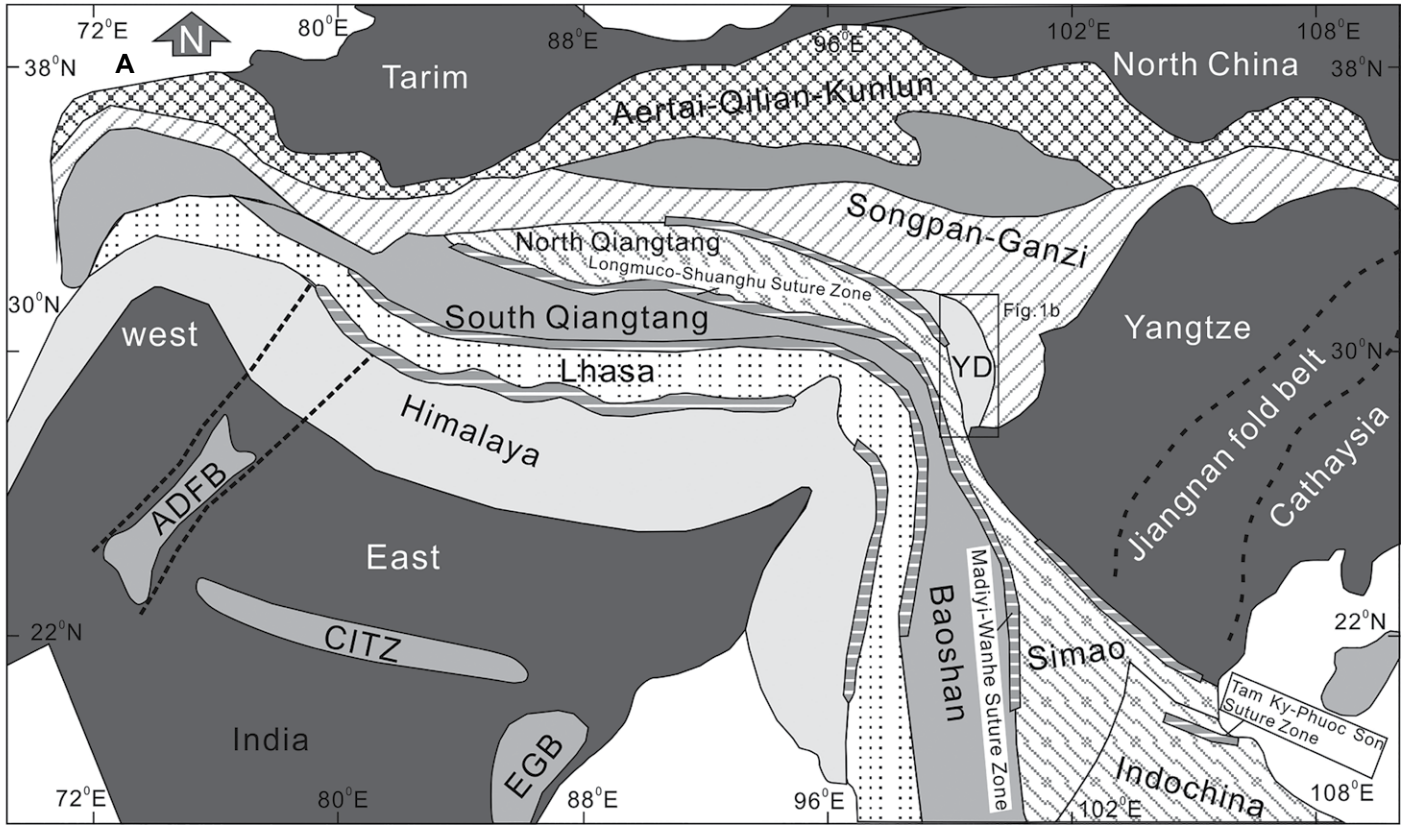


Figure 1. Simplified geological maps show (A) the Tibetan Plateau (after Tian et al., 2020), (B) the Yidun terrane (after Peng et al., 2014), (C) the Gongling region of the Eastern Yidun subterrane (after BGMRS, 1980, 1984), and (D) the Cryogenian–Ordovician strata and samples in the Gongling region (modified from BGMRS, 1980, 1984). ADFB—Aravalli-Delhi fold belt; CITZ—Central Indian tectonic zone; EGB—East Ghats belt; EYD—Eastern Yidun subterrane; WYD—Western Yidun subterrane.

the Jiangnan–Aravalli–Delhi fold belt separating the Yangtze–Marwar block from the Cathaysia–Bundelkhand block in the interior.

GEOLOGICAL SETTING AND SAMPLES

South China was formed by the amalgamation of the Yangtze block to the northwest and the Cathaysia block to the southeast along the Neoproterozoic Jiangnan fold belt (Zhao et al., 2011; Cawood et al., 2018). To the north of South China is the North China craton and to the southwest is the Indochina block. They are separated by the Qinling–Dabie–Sulu orogen and the Ailaoshan–Song Ma suture zone, respectively (Fig. 1). South China is bounded by the Yidun and Songpan–Ganzê terranes of the Tibetan Plateau to the northwest, which are separated by the Longmenshan Fault (Fig. 1). The geological characteristics of the Yangtze and Cathaysian blocks have been summarized in detail by some authors (e.g., Cawood et al., 2013, 2018; Zhao et al., 2018b; Chen et al., 2021).

The Yidun terrane, a microcontinent located between the Qiangtang and Songpan–Ganzê terranes, is considered to have been part of the Yangtze block before the Mesozoic (BGMRS, 1980, 1984). It is surrounded by two Paleoproterozoic suture zones, the Jinshajiang suture to

the west and the Ganzê–Litang suture to the east (Figs. 1A–1B; BGMRS, 1984; Peng et al., 2014). To the southeast of the Yidun terrane is the Yangtze block, which is separated by the Longmenshan–Jinhe Fault (BGMRS, 1984; Peng et al., 2014). Based on the tectono-stratigraphical distinction of the two flanks of the north–south-trending Xiangcheng–Geza Fault, the Yidun terrane can be divided into the Western Yidun subterrane (also known as the Zhongza massif; Peng et al., 2014) and the Eastern Yidun subterrane (Figs. 1A–1B; Peng et al., 2014).

The western subterrane consists mainly of greenschist to lower amphibolite facies Paleozoic meta-sedimentary rocks intercalated with minor meta-volcanics (BGMRS, 1984; Pan et al., 2004). The eastern subterrane is dominated by Triassic volcano-clastic rocks with minor Neoproterozoic–Paleozoic sedimentary successions in the southeast (BGMRS, 1984; Tian et al., 2018). The oldest strata are greenschist–amphibolite facies Neoproterozoic Qiasi Group exposed in the southeast region of the Eastern Yidun subterrane, which comprise a suite of metamorphosed Neoproterozoic volcano-sedimentary successions consisting of meta-volcanic schist, leptynite, and marble (Fig. 1; BGMRS, 1984; Tian et al., 2018). The strata can be divided into four segments from bottom to top based on their lithological characteristics (Figs. 1C–1D; BGMRS, 1984). Unconformably overlying the Qiasi Group are late Neoproterozoic (Ediacaran) sequences comprising sandstone, carbonate, and dolostone (BGMRS, 1984). In turn, these strata are unconformably overlain by Early Cambrian meta-sediments that consist of a sequence of schist, phyllite, and carbonate (BGMRS, 1984; Pan et al., 2004). Ordovician succession, including sandstone, siltstone, and slate (Figs. 1C–1D; BGMRS, 1984; Pan et al., 2004), unconformably overlies Lower Cambrian strata, and is in turn unconformably overlain by Early Silurian slate and silicalite (Du, 1986; Pan et al., 2004). Above these strata are upper Paleozoic sedi-

mentary rocks comprised of Devonian schist, marble, and sandstone, Carboniferous–Upper Permian limestone, Upper Permian basalt, and slate (BGMRS, 1984). These Upper Paleozoic strata are unconformably overlain by Mesozoic and Paleogene sedimentary rocks in some places (Fig. 1C; BGMRS, 1984; Pan et al., 2004). In addition, voluminous Middle–Late Triassic (230–206 Ma) and minor amounts of Permian, Cretaceous, and Cenozoic igneous rocks are exposed in the Eastern Yidun subterrane (e.g., BGMRS, 1984; Hou et al., 2001, 2004; Reid et al., 2007; Wang et al., 2013a; Peng et al., 2014).

A total of five samples were collected for zircon U–Pb dating and Hf isotope analyses (Table 1 and Figs. 1–2). Two schist samples (10YD-93 and 10YD-97) were collected from the fourth and third segments of the Qiasi Group, respectively (Table 1 and Figs. 1–2). One sandstone sample (10YD-100) was collected from the Ediacaran Dengying Formation; a slate sample (10YD-102) and a schist sample (10YD-99) were collected from the Ordovician strata (Table 1 and Figs. 1–2).

ANALYTICAL METHODS

Laser Ablation–Inductively Coupled Plasma–Mass Spectrometry (LA–ICP–MS) Zircon U–Pb Dating

Ca. 5 kg of each sample was crushed and milled, and then zircons were separated using heavy-liquid and magnetic methods at the Laboratory of the Geological Team of Hebei Province, China. Cathodoluminescence (CL) images were taken at the Guangzhou Institute of Geochemistry, Chinese Academy of Sciences (GIG–CAS) to inspect the internal structures of individual zircons and select positions for U–Pb and Lu–Hf isotope analyses. Detrital zircons of varying size and shape were selected randomly, and grains with obvious cracks or inclusions were excluded.

TABLE 1. SAMPLE LOCATIONS AND STRATIGRAPHIC INFORMATION

Sample	Lithology	Latitude (°N)	Longitude (°E)	Stratigraphic age	Mineral composition	Petrographical descriptions
10YD-93	Schist	28°21.655	100°13.619	The fourth member of Qiasi Group (Ptq ⁴ ; Cryogenian)	Quartz (80–85%), mica (5–10%), lithic fragment (1–5%) and minor heavy minerals	Fine-grained, subangular to subrounded, moderately to well sorted, grain-supported, moderate textural maturity
10YD-97	Schist	28°22.453	100°14.064	The third member of Qiasi Group (Ptq ³ ; Cryogenian)	Quartz (40–50%), mica (35–40%), and minor heavy minerals	Fine-grained, subangular to subrounded, moderately sorted, grain-supported, moderate textural maturity
10YD-99	Schist	28°23.193	100°14.410	Wachang Formation (O ₁)	Quartz (60–65%), mica (20–35%), and minor heavy minerals	Fine-grained, subangular to subrounded, moderately to well sorted, grain-supported, moderate textural maturity
10YD-100	Sandstone	28°24.153	100°14.546	Dengying Formation (Ediacaran)	Quartz (70–80%), feldspar (10–15%), and minor heavy minerals	Middle- and fine-grained, angular to subangular, moderately to poorly sorted, grain-supported, moderate to low textural maturity
10YD-102	Slate	28°24.958	100°14.405	Wachang Formation (O ₁)	Quartz (~70%), mica (20–25%), and minor heavy minerals	Fine-grained, subangular to subrounded, moderately sorted, matrix-supported, moderate textural maturity

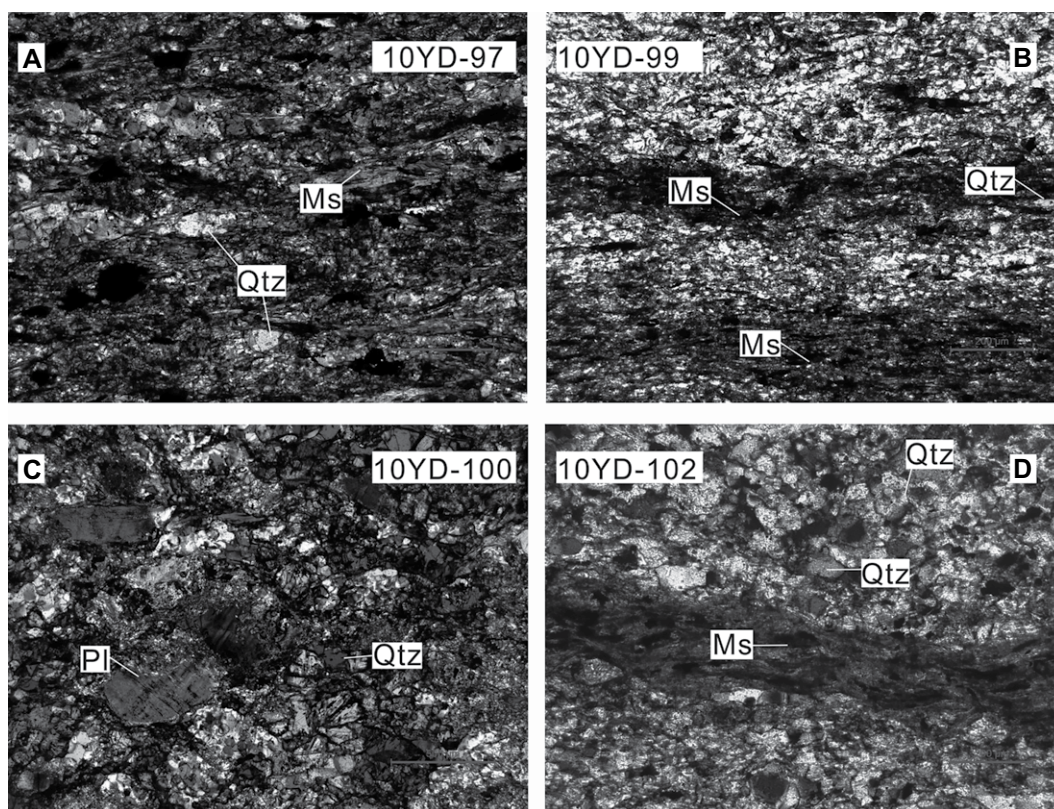


Figure 2. Photographs of the representative (meta-)sedimentary samples from the Eastern Yidun subterrane are shown. (A–B) The schist samples, (C) the sandstone sample, and (D) the slate sample. Qtz—quartz; Pl—plagioclase; Ms—mica.

In situ zircon U-Pb dating was carried out using an Agilent 7700× ICP-MS coupled to a 193 nm ArF excimer laser ablation system (GeoLas 2005, Lambda Physik) housed at the Jupu Analysis Lab in Nanjing, China. Analytical procedures were the same as those described by Liu et al. (2010). The frequency of the laser system was 10 Hz. Gas flow rate, with highly purified He as the carrier gas, was 0.7 L/mn; the flow rate of auxiliary gas Ar was 1.13 L/mn. The spot diameter was 40 μm in size. A total acquisition time for one spot was 45 s. Zircon 91500 was used as the external standard for U-Pb dating and was analyzed twice every five analyses. Time-dependent drifts of U-Th-Pb isotopic ratios were corrected using a linear interpolation (with time) for every five analyses according to the variations of 91500 (i.e., 2 zircon 91500 + 5 samples) (Liu et al., 2010). Zircon 91500 yielded an average $^{206}\text{Pb}/^{238}\text{U}$ age of 1062 ± 10 Ma (2σ ; MSWD = 0.01, $n = 101$), which is within error of its recommended age (1064.2 ± 1.7 Ma; Yuan et al., 2004). Analysis of the secondary zircon standard, GJ-1, gave a weighted mean $^{206}\text{Pb}/^{238}\text{U}$ age of 599.6 ± 4.3 Ma (2σ ; MSWD = 2.4, $n = 12$), which is within error of the accepted value (599.8 ± 1.7 Ma). Correction of common lead followed the method described by Liu et al. (2010). Data were processed with the ICPMS-DataCal program (Liu et al., 2010). Uncertainties on individual analyses in data tables were

reported at a 2σ level. Results were analyzed and plotted using Isoplot 3.0 (Ludwig, 2003). Zircon ages younger than 1000 Ma were based on $^{206}\text{Pb}/^{238}\text{U}$ ratios, and ages older than 1000 Ma were based on $^{207}\text{Pb}/^{206}\text{Pb}$ ratios. In this study, we excluded zircon age analyses with >10% discordance (Dickinson and Gehrels, 2009).

In Situ Zircon Hf Isotope Analysis

After the LA-ICP-MS zircon U-Pb dating, zircon Lu-Hf isotope compositions were analyzed by a 193 nm Ar-F excimer laser ablation system (RESOLUTION M-50-LR) attached to a multi-collector ICP-MS (Neptune Plus), at GIG-CAS. The Hf isotopes were obtained with a beam diameter of 45 μm, pulse rate of 6 Hz, energy density of 80 J/cm², and ablation time was 29 s. Quality control was ensured by measuring zircon standard Penglai for the unknown samples during the analyses to evaluate the reliability of the analytical data. This yielded a weighted mean average $^{176}\text{Hf}/^{177}\text{Hf}$ ratio of 0.282908 ± 0.000004 (2σ ; $n = 88$), which is consistent within errors with the reported values of 0.282906 ± 0.000010 (Li et al., 2010). In situ Hf isotope measurements were subsequently conducted on the same spots or the same age domains for age determinations of the concordant grains as guided

by CL images. The initial Hf isotopic ratios and crustal model ages were calculated using the dating results of the same spots.

RESULTS

Zircon U-Pb Geochronology

The LA-ICP-MS U-Pb dating results of zircons for the studied samples are listed in Table S1¹. Most analyses were plotted on or near the concordia curve (Fig. 3). The late Neoproterozoic and Ordovician samples in the Eastern Yidun subterrane show distinguishable age spectra. For example, the late Neoproterozoic samples display a unimodal pattern, whereas the Ordovician samples show a multimodal pattern (Fig. 3).

¹Supplemental Material. Table S1: Detrital zircon U-Pb ages from the Neoproterozoic to Early Paleozoic sequences in Eastern Yidun subterrane. Table S2: Lu-Hf isotopes of detrital zircons from the Neoproterozoic to Early Paleozoic sequences in Eastern Yidun subterrane. Figure S1: CL images of representative zircons from the Neoproterozoic to Early Paleozoic sequences in Eastern Yidun subterrane. The red and yellow circles represent the spot location for LA-ICP-MS U-Pb dating and Hf isotopic analyses, respectively. Please visit <https://doi.org/10.1130/GSAB.S.19404038> to access the supplemental material, and contact editing@geosociety.org with any questions.

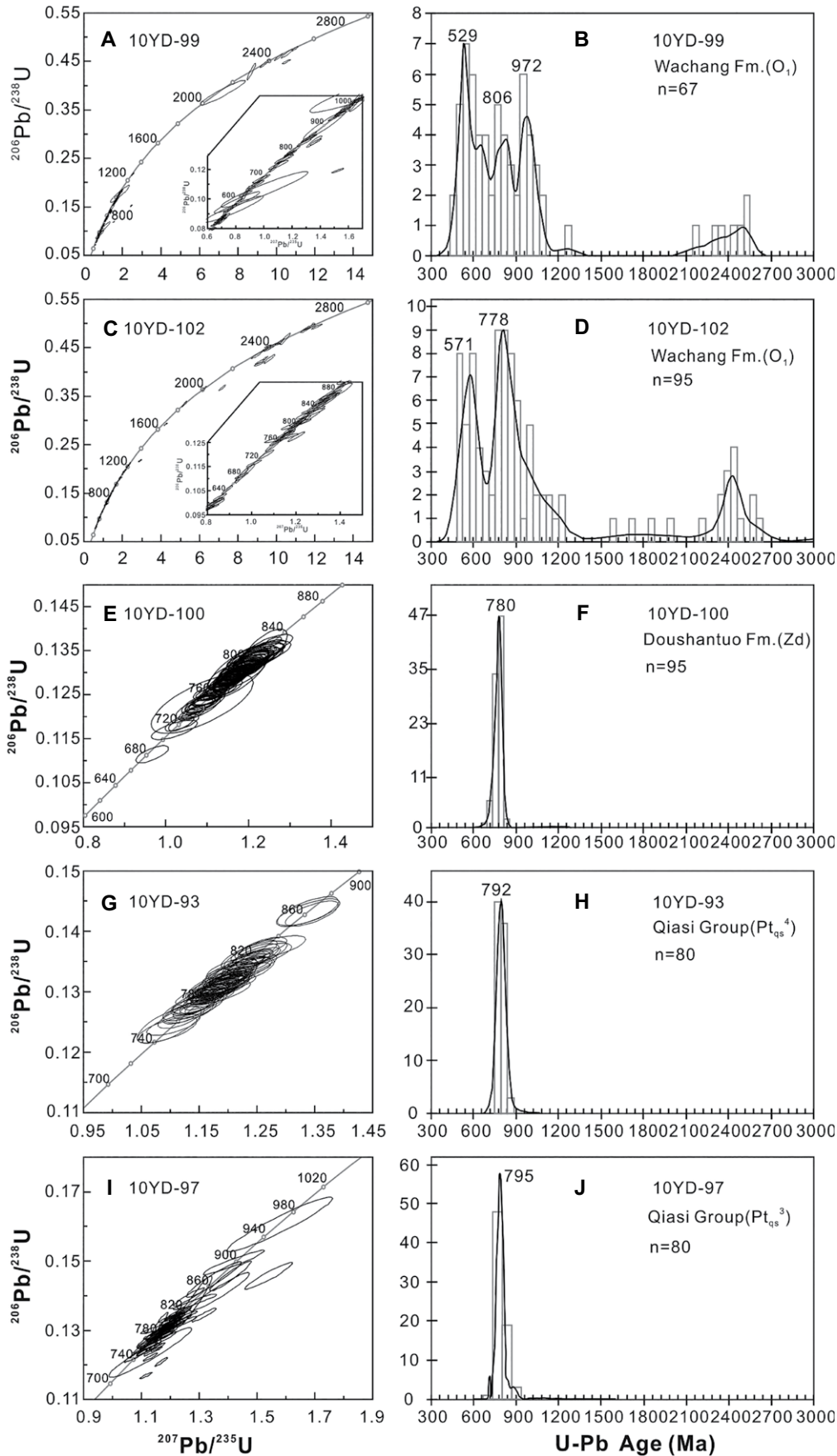


Figure 3. Detrital zircon U-Pb concordia and age spectra diagrams of the Neoproterozoic–Ordovician samples from the Eastern Yidun subterrane are shown.

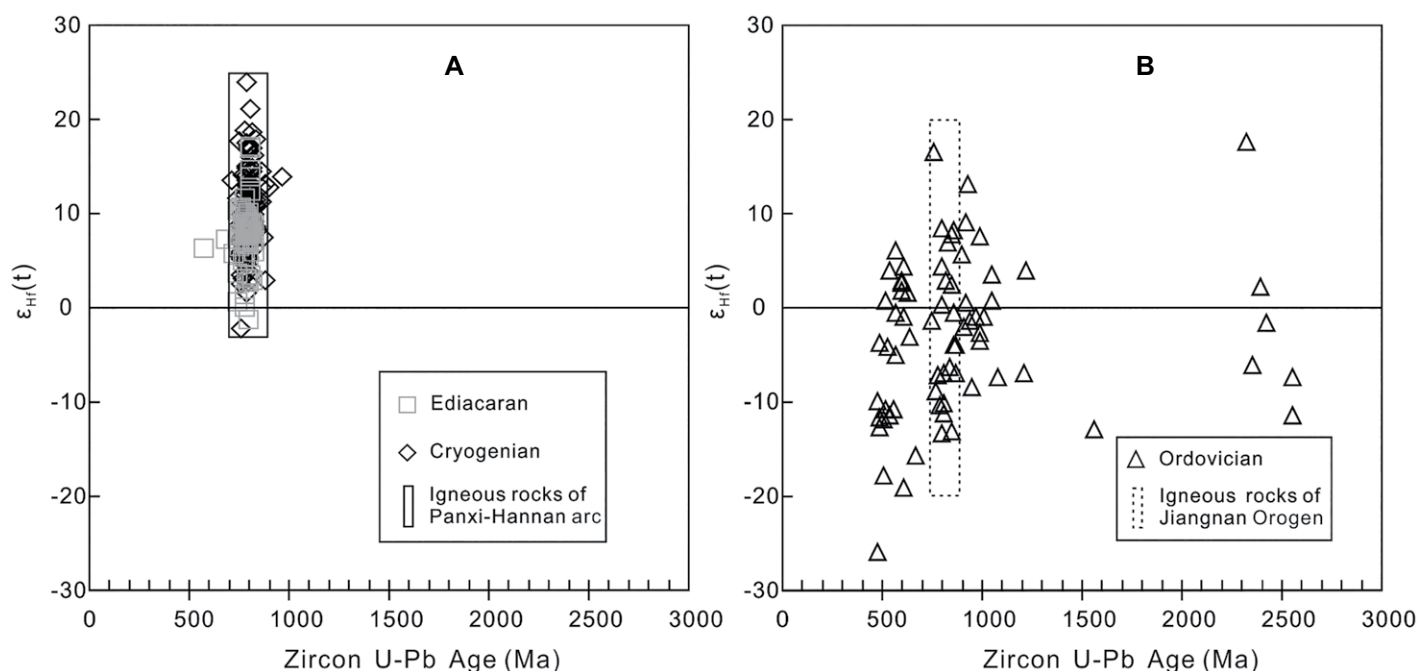


Figure 4. Zircon $\epsilon_{\text{Hf}}(t)$ versus U-Pb age plots of the (A) Neoproterozoic and (B) Ordovician detrital sediments in the Eastern Yidun subterrane are shown. The detrital zircon $\epsilon_{\text{Hf}}(t)$ data from the Yidun terrane are from this study and Tian et al. (2020). The igneous zircon $\epsilon_{\text{Hf}}(t)$ values of the Panxi-Hannan arc are from Zhao et al. (2010, 2017); Zhao et al. (2008b); Li et al. (2018); Ao et al. (2019); Zhu et al. (2019a); and Qi and Zhao (2020). The igneous zircon $\epsilon_{\text{Hf}}(t)$ values of the Jiangnan orogen are from Yao et al. (2019, and references therein).

Zircon grains from all of the Neoproterozoic samples in the Eastern Yidun subterrane are primarily euhedral and partly subeuhedral. All show magmatic oscillatory zoning in CL images (Fig. S1; see footnote 1), and 278 out of 280 analyses produced 90–100% concordant ages, which are considered in the following discussion. They give an age spectrum ranging from 960 Ma to 574 Ma, and each sample displays a similar unimodal pattern with a single major age population at 800–760 Ma (Table S1 and Fig. 3). Only one older age of ca. 960 Ma is present in the sample 10YD-97 (Table S1 and Fig. 3).

Most zircon crystals from the Ordovician samples in the Eastern Yidun subterrane are subeuhedral to subround, while some grains are rounded. All of the zircons analyzed show magmatic oscillatory zoning in CL images (Fig. S1), and 163 out of 165 analyses have less than 10% discordance, which is considered in the following discussion. The two Ordovician samples yield U-Pb ages varying from 3093 Ma to 447 Ma. They share similar multimodal distribution patterns, with major age populations at 600–500 Ma and 860–700 Ma and a subordinate age group at 2500–2400 Ma (Fig. 3). One difference is that the schist sample (10YD-99) has an alternative Grenvillian age population of 1100–900 Ma (Fig. 3).

Zircon Hf Isotopic Compositions

A total of 230 analyses of these three Neoproterozoic samples from the Eastern Yidun subterrane exhibit a wide range of initial $^{176}\text{Hf}/^{177}\text{Hf}$ ratios ranging from 0.282248 to 0.283031 (Table S2; see footnote 1). Among them, 228 spots have positive $\epsilon_{\text{Hf}}(t)$ values between +0.1 and +24.0 with T_{DM}^{C} ages at 1.57–0.77 Ga (Table S2 and Fig. 4), which are compatible with those of the Neoproterozoic igneous rocks along the western and northern margins of the Yangtze block (Zhao et al., 2018c, 2021b). Only two Neoproterozoic zircons give slightly negative $\epsilon_{\text{Hf}}(t)$ values of –2.1 and –1.2, respectively (Table S2 and Fig. 4).

In the case of the Ordovician samples in the Eastern Yidun subterrane, a total of 75 analyses exhibit a wide range of initial $^{176}\text{Hf}/^{177}\text{Hf}$ ratios ranging from 0.280824 to 0.282793 and large variations of $\epsilon_{\text{Hf}}(t)$ values (–25.9 to +35.0), which are different from those Neoproterozoic samples from this study that are dominated by positive $\epsilon_{\text{Hf}}(t)$ -value zircons (Table S2 and Fig. 4). The samples from the main age group of 650–500 Ma have similar $\epsilon_{\text{Hf}}(t)$ values (–25.0 to +6.1) as those of the magmatic rocks in the Kuunga orogen (Zhu et al., 2011, and references therein), while the age cluster at 830–700 Ma yields similar $\epsilon_{\text{Hf}}(t)$ values (–13.4 to +16.5) as

those of the coeval igneous rocks in the Jiangnan orogen in South China (Fig. 4; Yao et al., 2019). The 1100–900 Ma detrital zircons from the schist sample (10YD-99) show $\epsilon_{\text{Hf}}(t)$ values ranging from –8.5 to +13.2, which are compatible with those in the Eastern Ghats orogen and Central Indian tectonic zone (Zhu et al., 2011; Bhowmik et al., 2012, and references therein). Minor ca. 2400 Ma zircons have variable $\epsilon_{\text{Hf}}(t)$ values between –11.4 and +35.0.

DISCUSSION

Sedimentary Provenance

By comparison, a unimodal pattern of the Neoproterozoic schists in the Eastern Yidun subterrane that is similar to those in the western Yangtze block reflects a common provenance (Fig. 5). Owing to the absence of the Neoproterozoic moderately felsic magmatic rocks within the Yidun terrane (Tian et al., 2020), these Neoproterozoic detrital materials cannot be sourced from the interior of this terrane. In contrast, they likely originated from 0.86 Ga to 0.70 Ga igneous rocks that are widely exposed along the northern and western margins of the Yangtze block, such as the Neoproterozoic Panxi-Hannan arc (Zhou et al., 2006; Zhao et al., 2018c, 2021b). Moreover, the Hf isotopic

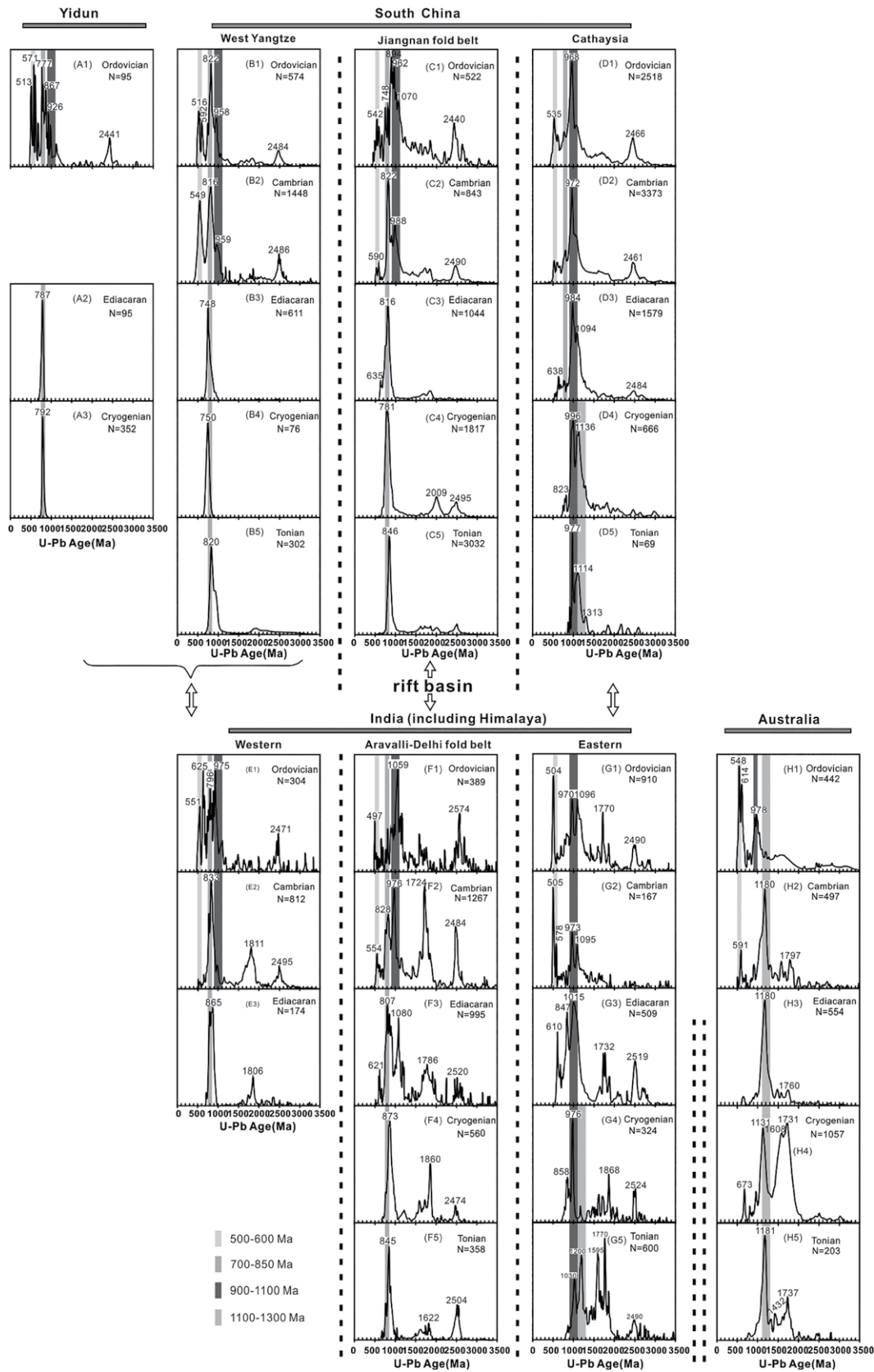


Figure 5. Detrital zircon age distributions are plotted for late Tonian to Ordovician sedimentary rocks from Yidun, South China, India, and Australia. Data sources: this study; DeCelles et al., 2000; Gehrels et al., 2006, 2011; Wang et al., 2007b; Malone et al., 2008; Sun et al., 2008, 2009; Long et al., 2011; Wang et al., 2010; Wu et al., 2010; Myrow et al., 2010; Xiang and Shu, 2010; Yu et al., 2010; Hofmann et al., 2011, 2016; Hughes et al., 2011, 2019; McKenzie et al., 2011, 2013; Yao et al., 2011; Wang et al., 2012a, 2012b, 2013b; McQuarrie et al., 2013; Xu et al., 2013, 2014; Wang et al., 2014; Turner et al., 2014; Yao et al., 2014, 2015; Cui et al., 2015; Chen et al., 2016, 2018, 2021; Wang et al., 2015; Yan et al., 2015; Yang et al., 2015; Haines et al., 2016; Johnson et al., 2016; Xia et al., 2016; Han et al., 2017; Wang et al., 2017b; Sun et al., 2018; Wang et al., 2018a, 2018b, 2018c; Zhao et al., 2018d; Zhang et al., 2018; Zhou et al., 2018b; Qasim et al., 2018; Qi et al., 2018, 2020; Liu et al., 2019a, 2019b, 2019c; Ma et al., 2019; Mukherjee et al., 2019; Wang et al., 2019a; Xiong et al., 2019; Xue et al., 2019; Yan et al., 2019; Yang and Jiang, 2019; Zhang et al., 2019a, 2019b; Zhu et al., 2019b; He et al., 2020; Keeman et al., 2020; Lan et al., 2020; Liu et al., 2020b; Luo et al., 2020; Mulder et al., 2020; Tian et al., 2020; Yuan et al., 2021a; Zhang et al., 2020b; Verdel et al., 2021; and Zhao et al., 2021a.

compositions of detrital zircons from these Neoproterozoic samples are in good agreement with those of magmatic zircons of the Neoproterozoic igneous rocks in the Panxi-Hannan arc (Fig. 4). In addition, these detrital zircons of our Neoproterozoic samples are euhedral with magmatic zoning (Fig. S1), which indicates a short-distance transport from its provenance. Hence, we suggest that the Neoproterozoic detritus in the Eastern Yidun subterrane was predominantly sourced from the coeval igneous rocks in the Panxi-Hannan arc along the western and northern margins of the Yangtze block.

In the case of the Ordovician samples, they show a multimodal pattern that is distinguishable from the unimodal one of the Neoproterozoic samples (Fig. 3). Except for sharing a main age of ca. 0.83–0.70 Ga with the Neoproterozoic samples, they have main age groups at ca. 0.65–0.50 Ga and ca. 1.00–0.90 Ga and a subordinate age group at ca. 2.40 Ga (Fig. 3). Alternatively, the 0.83–0.70 Ga zircons of the Ordovician samples have distinguishable $\epsilon_{\text{Hf}}(t)$ values (–16.1 to +15.7) from those of the Neoproterozoic samples (Table S2), but they are similar to those of the coeval igneous rocks in the Jiangnan orogen in South China as mentioned before (Fig. 4; Yao et al., 2019). Taken together, it is obvious that the 0.83–0.70 Ga zircons of the Ordovician samples could not originate mainly from the erosion of the Panxi-Hannan arc magmatic rocks in the western Yangtze block. In contrast, it is possible that most of the 0.83–0.70 Ga zircons in the Ordovician sediments in the Eastern Yidun subterrane were derived from the Jiangnan orogen. Concerning the 1.00–0.90 Ga and 0.65–0.50 Ga detrital zircons, they were surprisingly sourced from the coeval igneous rocks of the South China interior; this is remarkable due to the absence of synchronous moderately felsic magmatic rocks within South China. Therefore, they could be exotic, having been transported long distance or recycled from the old strata in South China (Cawood et al., 2018), which are consistent with the subrounded and rounded attributes of these detrital zircons (Fig. S1). Indeed, the Ordovician sediments in the Eastern Yidun subterrane share a similar age spectrum and zircon Hf isotopic compositions as the Cambrian unit in the western Yangtze block (Chen et al., 2021), which indicates that the former could be primarily derived from the recycling of the latter. But the ultimate sources of the 1.00–0.90 Ga and 0.65–0.50 Ga detrital zircons are the Eastern Ghats–Rayner Complex and the Kuunga orogen located in the eastern India region, while the 0.83–0.70 Ga zircons are from the Jiangnan orogen in South China.

Tectonic Link Between South China and India

Two contrasting reconstruction models have been proposed for the paleogeographic position of South China in Rodinia: an internal location within the Rodinia supercontinent versus an external setting along the margin of the Rodinia supercontinent (e.g., Li et al., 1999, and references therein; Zhao and Cawood, 1999; Cawood et al., 2018). For the internal model, South China was located between the Laurentian and Australian blocks (e.g., Li et al., 1999; Li et al., 2002). In the peripheral model, South China was attached to India in the early to mid-Neoproterozoic (e.g., Cawood et al., 2018; Zhao et al., 2018b, 2021a).

In fact, increasing lines of evidence that include magmatic, paleomagnetic, and sedimentary data (e.g., Yang et al., 2004; Gregory et al., 2009; Yao et al., 2014; Wang et al., 2017a, 2021; Cawood et al., 2018; Zhao et al., 2018b; Chen et al., 2021) demonstrate that South China was located to the periphery of Rodinia rather than in its interior during Neoproterozoic time. Nonetheless, the spatio-temporal evolution of South China within these peripheral models previously proposed from Rodinia to Gondwana is also different. For example, based on the paleomagnetic studies of the Middle Cambrian sediments from the western Yangtze block, Yang et al. (2004) proposed that South China was connected to NW Australia from latest Proterozoic and early Paleozoic time until its breakup from Australia in the middle Devonian. In contrast, after comparing detrital zircon age spectra of the Gondwana-derived blocks/terraces, Yao et al. (2014) suggested that the Cathaysia side of South China was closely linked with the northern margin of India (the Himalaya region) by the Ediacaran–Cambrian collision between South China and India and persisted until the opening of the Paleo-Tethys Ocean during Devonian time. In recent years, after comparing the magmatism, sedimentation, bio-stratigraphic affinity, and paleomagnetic pole of South China with those of India and Australia, some researchers concluded that South China was most likely close to northern India during Neoproterozoic and even early Cambrian times but was progressively separating from the latter, and rotating and migrating along the Gondwanan margin toward northeastern India and NW Australia during latest Ediacaran or early Cambrian time (e.g., Jiang et al., 2003; Chen et al., 2021).

However, the Tonian to Cambrian strata on the Cathaysia block and on the western Yangtze block show similar age spectra (Fig. 5), indicating that their respective detrital provenance did not change with time. In other words, they

each shared a common source from the Tonian to Cambrian although their provenance is different because the Cathaysia block has a different main age group at ca. 960 Ma from the western Yangtze block at ca. 800 Ma (Fig. 5). This, in turn, hints that the tectonic setting for the Tonian to Cambrian sedimentation in these two blocks did not change. Accordingly, it is unlikely that the Yangtze block commenced to rift from northwestern India since the late Tonian, and South China was migrating toward NW Australia. Moreover, the absence of the diagnostic ca. 1170 Ma age group of NW Australia in the Tonian to early Paleozoic strata in the Cathaysia block (Fig. 5; e.g., Wang et al., 2010; Yao et al., 2014) also argues against a close proximity to NW Australia during late Neoproterozoic to early Paleozoic time. By contrast, the presence of a predominant age population of detrital zircons at ca. 960 Ma from the Tonian to Cambrian strata in the Cathaysia block (Fig. 5; e.g., Wang et al., 2010; Yao et al., 2014) suggests that a common northern Indian (the Tethyan sequences) provenance had continuously provided the detritus input into the Cathaysia block from the Tonian to Cambrian. In fact, the similarities in facies assemblages of the late Neoproterozoic–early Cambrian sedimentary rocks between South China and India also lend strong support to this proposition. For example, the Yangtze block of South China and NW India share similar late Tonian rift-related, siliciclastic-volcanic successions, Cryogenian glaciogenic diamictite successions, Ediacaran carbonate successions, and Early Cambrian phosphorite and clastic successions (Jiang et al., 2003). Correspondingly, the Cathaysia block and eastern India region contain similar Tonian siliciclastics, Cryogenian sandstones and diamictites, and Ediacaran–Cambrian siliciclastics (Wang and Li, 2003; Wang et al., 2021). As a consequence, we propose that South China remained closely linked with India and formed the South China–India Duo at least during late Tonian to early Cambrian time. Such a connection model has been proposed by Cawood et al. (2018) and Zhao et al. (2018b). South China finally separated from Indian Gondwana likely after the early Cambrian (ca. 510 Ma) due to the opening of the Proto-Tethys Ocean rather than the Paleo-Tethys Ocean after the Devonian (also see discussion in Implication for Breakup of South China from Gondwana).

Double Late Neoproterozoic Rift Systems Developed in the South China–India Duo

Increasing lines of evidence, such as comparable Neoproterozoic rift-related magmatism and sedimentation of the Jiangnan fold belt in South China and that of the Aravalli-Delhi fold

belt in NW India, illustrate the development of a Neoproterozoic intracontinental linear rift basin in the interior of the South China–India Duo (Fig. 6; Wang and Li, 2003; Wang et al., 2017a; Zhao et al., 2018b, and references therein). For example, from a sedimentation perspective, some coeval extension-related basins with similar lithological assemblages and sedimentary sequences had developed in the Sindreh and Punagarh basins along the western margin of the Aravalli–Delhi fold belt in NW India (Jiang et al., 2003; Zhao et al., 2018b, and references therein), the unnamed basin in the Lesser Himalaya north of the Aravalli–Delhi fold belt (i.e., the Jaunsar–Simla and Blaini sequences; Jiang et al., 2003; Zhao et al., 2018b, and references therein), and the Nanhua rift basin in South China (Wang and Li, 2003; Zhao et al., 2018b). In addition, the late Tonian–Ediacaran sedimentary sequences in the Jiangnan and Aravalli–Delhi fold belts share similar detrital zircon age patterns and overlapping $\epsilon_{\text{Hf}}(t)$ values (Fig. 5; Wang et al., 2017b; Wang et al., 2021), which also favors the idea of depositional continuity in the Jiangnan–Aravalli–Delhi fold belt at that time. Besides, similar Neoproterozoic rift-related magmatism, including bimodal magmatic rocks and A-type granites that are generally produced in extension-related regimes, has been identified in the Malani Igneous Suite located to the western margin of the NE-trending Aravalli–Delhi fold belt of NW India (e.g., Wang et al., 2017a; Zhao et al., 2018b; and references therein) and the Jiangnan fold belt in South China (e.g., Wang and Li, 2003; Deng et al., 2016; Li et al., 2008). More importantly, the recognition of late Neoproterozoic magmatic zircons (<5%) that have lower $\delta^{18}\text{O}$ than the mantle values ($5.3 \pm 0.6\text{‰}$; Valley et al., 1998) in these two aforementioned belts (Fig. 6; Wang et al., 2017a; Zhao et al., 2018b; Zhang et al., 2020a; Li et al., 2021, and references therein) indicates the development of synchronous rifting in NW India and the interior of South China (Zhao et al., 2018b).

In fact, an alternative Neoproterozoic extension-related tectonic zone had also developed simultaneously along the northern and western margins of the Yangtze block of South China. For instance, some Neoproterozoic extension-related igneous rocks developed along the northern–western margin of the Yangtze block, including the Tiechuanshan (ca. 820 Ma) and Suxiong (ca. 800 Ma) bimodal volcanic rocks, and the Daxiangling (ca. 816 Ma), Tiechuanshan, Huangguan and Mianning (780 Ma), and Panzhuhua (750 Ma) A-type granites, and low- $\delta^{18}\text{O}$ magmatic rocks (Fig. 6; e.g., Li et al., 2002; Wu et al., 2020; and references therein). Although a mantle plume setting has been invoked to account for such extension-related magmatism

(Li et al., 2002; Wang et al., 2007a), this scenario fails to explain the presence of more voluminous 820–770 Ma magmatic rocks in the Panxi–Hannan region on the northern and western Yangtze block that feature typical arc geochemical signatures (Zhao et al., 2011; Zhao et al., 2018b, and references therein). In contrast, a prolonged subduction-related arc environment as proposed by some authors (Zhou et al., 2006; Cawood et al., 2018; Zhao et al., 2018b, 2018c, 2021b) could be the most plausible explanation for the 820–770 Ma magmatism. Moreover, the arc-like geochemical characteristics and high proportion of Neoproterozoic detrital zircons (crystallization and depositional ages [CA–DA] <100 Ma in 30% of the zircon population; Fig. 7) of the Neoproterozoic sedimentary samples from the Yidun terrane also indicate deposition in a convergent setting basin (Cawood et al., 2012; Tian et al., 2020). In this respect, a back-arc environment is likely responsible for the coexistence of arc- and extension-type magmatic rocks on the western and northern margins of the Yangtze block, as was assumed by Luo et al. (2018). However, such a model is incompatible with the magmatic pattern of a back-arc environment, which is dominated by arc-type magmatic rocks with some extension-related rocks in this region as mentioned before (Cawood et al., 2018; Zhao et al., 2018b; Wu et al., 2020). In other words, these Neoproterozoic arc-type magmatic rocks should represent the important component of simultaneous continental arc. Moreover, considering that a huge thickness of extension-related late Neoproterozoic volcanoclastic sediments (>5 km) coexists with synchronous magmatic rocks on the northern and western margins of the Yangtze block and the southeastern margin of the Ganzê and Yidun terranes (BGMRSP, 1984; Zhou et al., 2006), we propose that intra-arc rifting is the most feasible explanation for such a coupling of magmatism and sedimentation. In fact, intra-arc rifting has been established in different subduction zones, such as northeast Japan in the west Pacific (Nakajima, 2013) and the Anglona region of northwestern Sardinia, Italy (Sowerbutts, 2000). In particular, the magmatic association and sedimentary pattern on the northern and western margins of the Yangtze block are similar to those in the intra-arc rift basin in the Anglona region of northwestern Sardinia, Italy (Sowerbutts, 2000).

As with the important parts of the Neoproterozoic subduction system on the western margin of Rodinia (e.g., Cawood et al., 2018; Zhao et al., 2018b; Wang et al., 2021), the coexistence of coeval, extension-related magmatic rocks and sedimentary basins with a large number of subduction-related, arc-type igneous rocks in Madagascar and Seychelles likewise indicates the

development of intra-arc rifting at that time. The rifting resembles that of the western and northern margins of the Yangtze block as stated above. For instance, the recognition of some mafic–ultramafic plutons with layered Fe–Ti–V oxide mineralization, A-type granitoids with a strongly alkaline composition and bimodal magmatic suite in the Imorona–Itsindro Suite of central Madagascar (Nédélec et al., 2016; Zhou et al., 2018a; and references therein), coupled with the same extensional structural signature as the ca. 790 Ma Imorona–Itsindro rocks and their country rocks (Nédélec et al., 2016, and references therein), were interpreted as due to continental rifting by Zhou et al. (2018a). Furthermore, from the perspective of a variation in isotopic composition, especially for zircon Hf and O isotopes of the 850–750 Ma magmatic rocks in central Madagascar, Zhou et al. (2018a) believed that synchronous continental rifting was involved in their petrogenesis. On the other hand, based on the fact that these central Madagascar rocks are dominated by calc-alkaline series and geochemically show an affinity to continental arc magmatic rocks, most researchers ascribed their generation to the effects of prolonged, Andean-like arc magmatism (Handke et al., 1999; Tucker et al., 1999; Kröner et al., 2000; Archibald et al., 2017; Armistead et al., 2019). In Seychelles, the 810–700 Ma magmatic rocks also display the coupling of typical Andean-type arc and rift-type (low- $\delta^{18}\text{O}$ granites) geochemical signatures (e.g., Ashwal et al., 2002, and references therein). Taken together, we propose that a late Neoproterozoic intra-arc rift system likely developed along the northern and western margins of the Yangtze block, through the Marwar terrane of western India, and then into Seychelles and Madagascar, although there are no such lines of evidence from western India yet (Fig. 6). Such an intra-arc rift system along the western margin of the South China–India Duo is different from the contemporaneous intracontinental one along the Jiangnan–Aravalli–Delhi fold belt within it (Fig. 6). Moreover, it can also account for the contradiction of the common presence of coeval arc-type and extension-related magmatic rocks coupled with some extension-related sedimentation in the same area.

The most plausible mechanism for the development of such double synchronous rift systems is the rollback of subducting oceanic slab beneath the South China–India Duo (Fig. 6), which would result in the asthenospheric upwelling and subsequent lithospheric extension at that time. The old suture belts, the Jiangnan fold belt between the Yangtze and Cathaysian blocks in South China (Zhao et al., 2011), and the Aravalli–Delhi fold belt between the Marwar and Bundelkhand terranes in NW

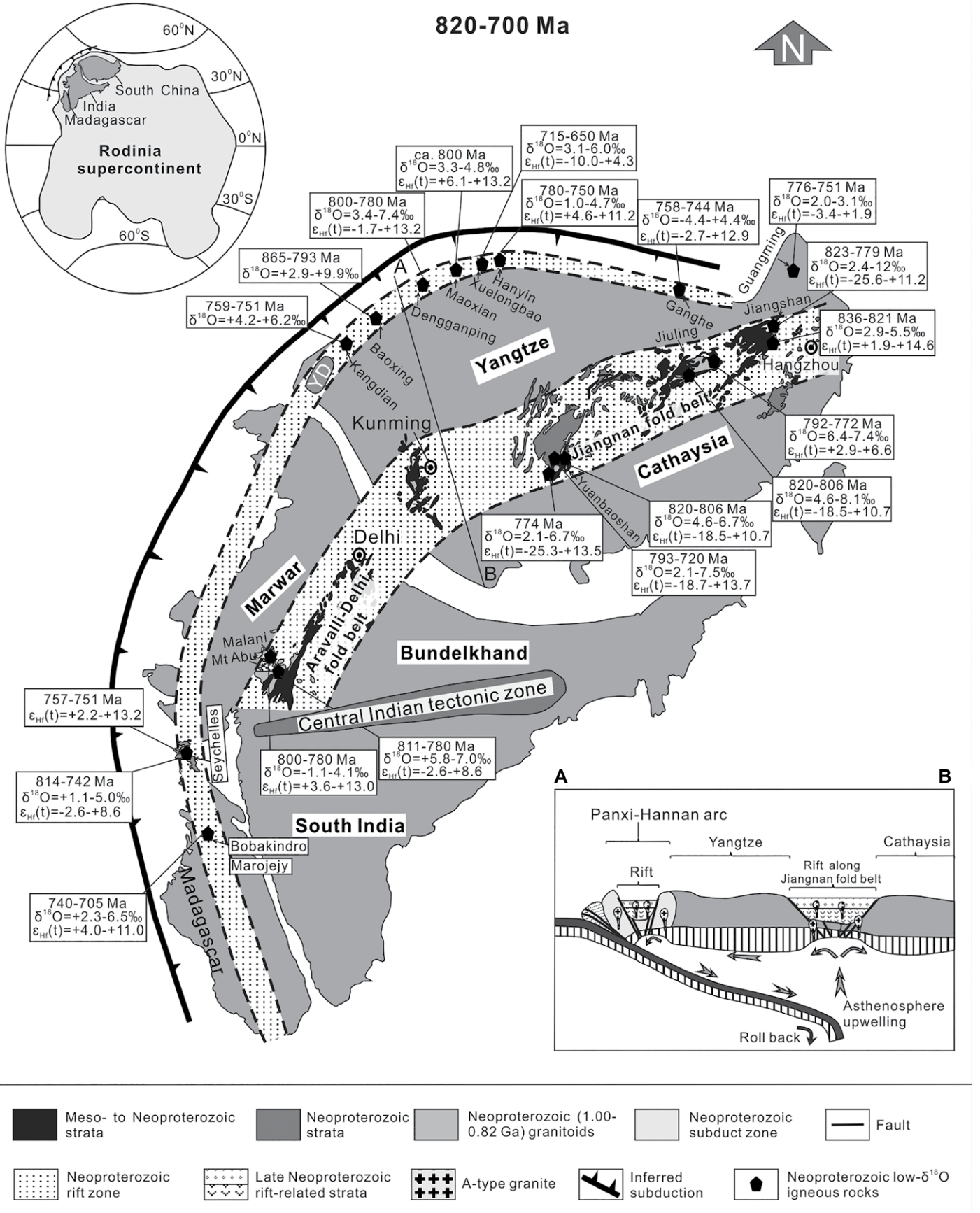


Figure 6. Diagram shows the proposed tectonic framework and paleogeographic positions for South China, India, Seychelles, and Madagascar in Rodinia during Neoproterozoic time (after Wang et al., 2017a, 2021; Cawood et al., 2018; Zhao et al., 2018b). YD—Yidun terrane. The zircon U-Pb age, $\epsilon_{\text{Hf}}(t)$, and $\delta^{18}\text{O}$ values of the Neoproterozoic igneous rocks in Madagascar, Seychelles, NW India, the Panxi-Hannan arc, and the Jiangnan-Aravalli-Delhi fold belt are from Harris and Ashwal (2002); Wang et al. (2011, 2012c, 2013c); Zhou et al. (2015a, 2015b, 2017); Yang et al. (2016); Wang et al. (2017a); Huang et al. (2018); Zhao et al. (2018b); Armistead et al. (2019); Jiang et al. (2020); Shellnutt et al. (2020); Qi and Zhao (2020); Wu et al. (2020); Zhou et al. (2020); Zou et al. (2020); and Yuan et al. (2021b).

India (Zhao et al., 2018b) are the most ideal areas for producing lithospheric extension. As a result, this is the most effective mechanism for inducing intracontinental rifting. An alternative region that is apt to trigger lithospheric extension is the continental arc, especially the intra-arc, where arc magmatism develops frequently and trans-lithospheric faults occur widely. Such a scenario could also be an important mechanism for the fragmentation of

some micro-continents/terrane/blocks from a big continent by intra-arc rifting.

Implication for Breakup of South China from Gondwana

Various researchers have proposed different breakup times for South China from Gondwana. For example, earlier studies suggested they separated from the Early Cambrian to Silurian in light of the variation in biogeography and stratigraphy in South China (Jiang et al., 2003, and references therein). Subsequently, considering the opening of the Paleo-Tethys Ocean between the South China and Indochina blocks, most workers believed that South China had broken up from Gondwana in the Devonian (e.g., Cawood et al., 2013; Metcalfe, 2013; Chen et al., 2021). Dating results of the remnant oceanic components provide critical evidence. The oldest plagiogranites at Shuanggou in the Jinshajiang-Ailaoshan Paleo-Tethys suture zone yielded zircon U-Pb ages of ca. 383–376 Ma (Jian et al., 2009). More recently, Wang et al. (2021) and Chen et al. (2021) compared the Neoproterozoic to early Paleozoic detrital zircon age spectra of South China with that of India and Australia and proposed that the initial separation of South China from NW India occurred in the Cryogenian and Early Cambrian, respectively. Moreover, based on the opening of the Paleo-

Tethys Ocean, they both concluded that South China should have finally drifted away from the northern margin of Australian Gondwana in the Devonian (Chen et al., 2021; Wang et al., 2021).

Regardless of how South China broke up from Gondwana, all of these views ignore a crucial fact, which is that the Proto-Tethys Ocean between South China and other Gondwana-derived blocks developed in the early Paleozoic. The opening of the Proto-Tethys Ocean should have led to the separation of South China from northern Gondwana. For instance, the early Paleozoic oceanic relics, including 477–460 Ma mid-oceanic-ridge basalt-type clinopyroxenite, gabbro, and amphibolite, and 519–502 Ma plagiogranites in the Tam Ky-Phuoc Son suture of Vietnam (Gardner et al., 2017; Nguyen et al., 2019, and references therein), indicate the presence of an early Paleozoic Ocean between the South China and Indochina blocks or South China–northern Indochina and the southern Indochina blocks (Fig. 1; Faure et al., 2018; Nguyen et al., 2019). On the other hand, another Proto-Tethys Ocean (518–438 Ma) between the South Qiangtang–Baoshan and North Qiangtang–Indochina terranes has been also documented in recent years (Fig. 1; Wu, 2013; Hu et al., 2014). In particular, the identification of the Cambrian ophiolites (ca. 517–490 Ma; Wu, 2013; Hu et al., 2014) implies the development of a Tethys Ocean at least in the Middle Cambrian. Thus, it is suggested that the Indochina block rifted away from the northern margin of Gondwana in the Middle Cambrian–Early Silurian interval. In turn, it is most plausible to infer that South China had separated from northern Gondwana at least by the Middle Cambrian to Early Silurian (Fig. 8; Liu et al., 2020a).

Whether South China was assembled with northern Gondwana by continent–continent collision similar to the collision between the South China and Indochina blocks in the late Silurian remains unknown (Faure et al., 2018; Nguyen et al., 2019). Although Zhang et al. (2014) proposed a continent–continent collision time of 427–422 Ma based on the study of high-pressure basic granulites in the central Qiangtang of Tibet, the identification of coeval (438 ± 11 Ma) oceanic cumulate gabbro in the same ophiolitic complex belt of central Qiangtang likely indicates that the early Paleozoic Proto-Tethys Ocean was not closed (Wu, 2013). In fact, no age-equivalent collision-related records have been discovered yet in the Changning–Menglian ophiolite belt, which represents the southern continuation of the central Qiangtang Proto-Tethys Ocean. More importantly, the identification of the early and late Paleozoic oceanic island basalt-type mafic rocks that had commonly experienced a similar Late Triassic ultrahigh-pressure metamorphism

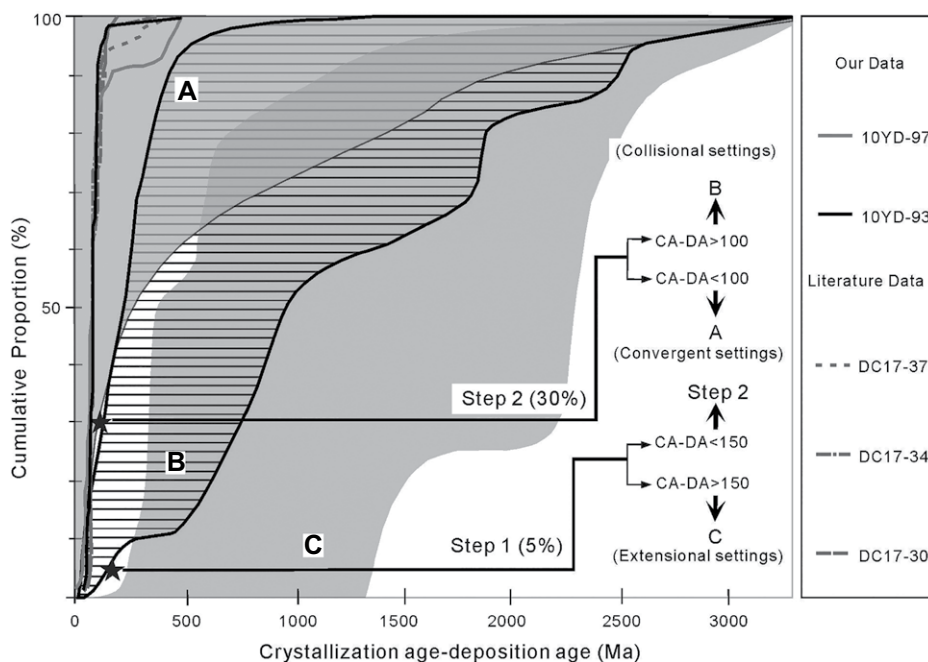


Figure 7. Depositional setting of the Cryogenian Qiasi Group in the Eastern Yidun subterrane is shown as inferred from a discrimination plot of cumulative proportions versus crystallization ages and depositional ages (CA–DA) of detrital zircons analyzed (modified from Cawood et al., 2012). Data are from this study and Tian et al. (2020).

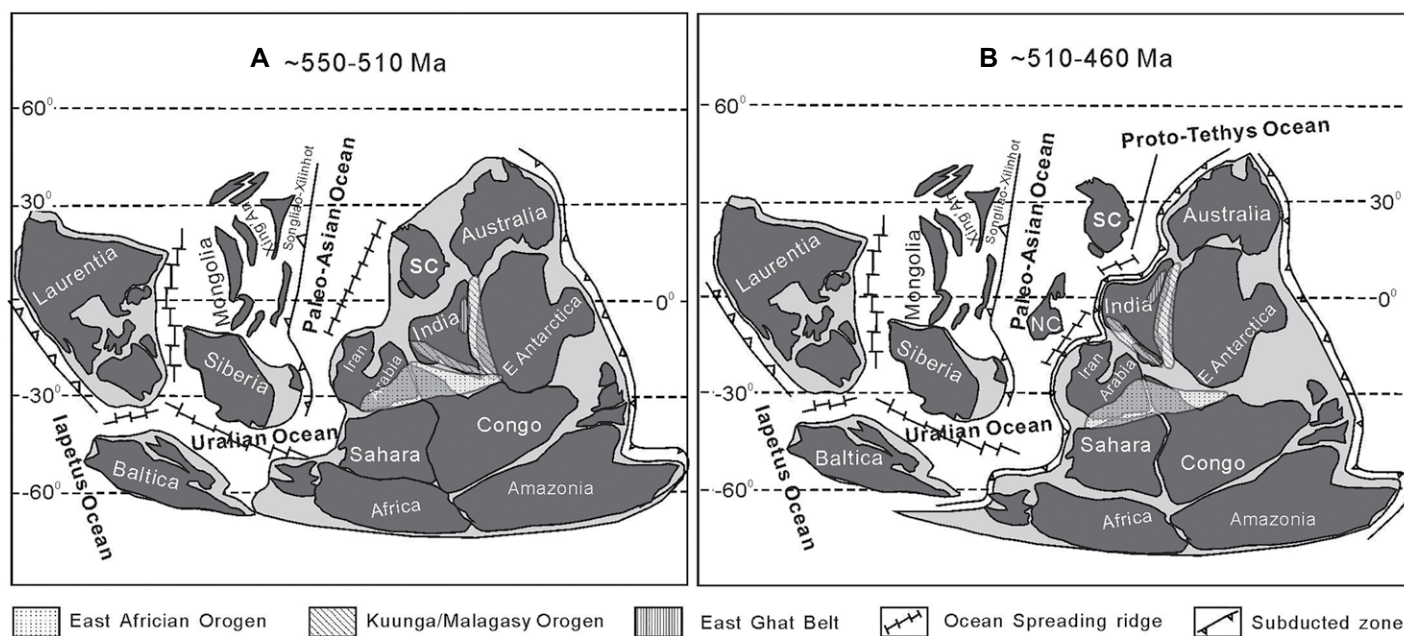


Figure 8. Tentative tectonic reconstruction models show South China (including the Yidun terrane) along with other ambient terranes in Gondwana during (A) late Ediacaran–Early Cambrian and (B) Middle Cambrian–Early Ordovician times (adapted from Zhao et al., 2018a). SC—South China; NC—North China.

(Fan et al., 2015) indicates that the Proto-Tethys Ocean could have developed persistently from the early Paleozoic to the end of the Paleozoic (Liu et al., 2020a, and references therein). Therefore, it is most likely that the Central Qiangtang high-pressure granulites within Tibet (Zhang et al., 2014) could be the products of early Paleozoic arc-continent collision during the tectonic evolution of a single Proto- and Paleo-Tethys Ocean. Considering all of the data (Chen et al., 2021, and references therein), we propose that the South China and Indochina blocks were separated from Indian Gondwana after the early Cambrian and were not welded to Gondwana again, although they were likely amalgamated together during late Silurian time (Faure et al., 2018; Nguyen et al., 2019) until the opening of the Paleo-Tethys Ocean between them (Jian et al., 2009).

CONCLUSIONS

The Neoproterozoic sediments in the Eastern Yidun subterrane were sourced mainly from the Panxi-Hannan magmatic arc on the northern and western margins of the Yangtze block while the Ordovician sequences were recycled from the Cambrian strata in the western Yangtze block.

South China kept a connection with India and formed the South China–India Duo located at the northwestern margin of Rodinia during late Tonian (ca. 830 Ma) to early Cambrian time.

Double late Neoproterozoic rift systems had developed in the South China–India Duo owing to the rollback of subducting oceanic slab beneath it, including an intra-arc rift along the northern and western margins of the Yangtze block through the Marwar terrane of western India, and then into the Seychelles and Madagascar terranes, and another coeval intracontinental one along the Jiangnan–Aravalli–Delhi fold belt within the interior of the South China–India Duo.

South China finally separated from northern India during middle Cambrian (ca. 510 Ma) to Ordovician time due to the opening of the Proto-Tethys Ocean but was not welded to Gondwana again.

ACKNOWLEDGMENTS

This work was jointly supported by the National Second Expedition to the Tibetan Plateau (2019QZKK0702) and National Natural Science Foundation of China (92055207, 42072263, 41490613, 41672058). We are also especially grateful to Science Editor Wenjiao Xiao, Associate Editor Changqing Yin and two anonymous reviewers for their constructive comments. This is a contribution from the Guangzhou Institute of Geochemistry, Chinese Academy of Sciences (GIG, CAS; No. IS-3137). All data of this manuscript will be available at the Mendelay Data repository (DOI: 10.17632/bs75p9fx6 h.3).

REFERENCES CITED

Ao, W.H., Zhao, Y., Zhang, Y.K., Zhai, M.G., Zhang, H., Zhang, R.Y., Wang, Q., and Sun, Y., 2019, The Neoproterozoic magmatism in the northern margin of the Yangtze block: Insights from Neoproterozoic (950–

706 Ma) gabbroic-granitoid rocks of the Hannan complex: *Precambrian Research*, v. 333, <https://doi.org/10.1016/j.precamres.2019.105442>.

Archibald, D.B., Collins, A.S., Foden, J.D., and Razakamanana, T., 2017, Tonian arc magmatism in central Madagascar: The petrogenesis of the Imorona-Itsindro Suite: *The Journal of Geology*, v. 125, no. 3, p. 271–297, <https://doi.org/10.1086/691185>.

Armistead, S.E., Collins, A.S., Merdith, A.S., Payne, J.L., Cox, G.M., Foden, J.D., Razakamanana, T., and Waele, B.D., 2019, Evolving marginal terranes during Neoproterozoic supercontinent reorganization: Constraints from the Bemarivo Domain in Northern Madagascar: *Tectonics*, v. 38, no. 6, p. 2019–2035, <https://doi.org/10.1029/2018TC005384>.

Ashwal, L.D., Demaiffe, D., and Torsvik, T.H., 2002, Petrogenesis of Neoproterozoic granitoids and related rocks from the Seychelles: The case for an Andean-type arc origin: *Journal of Petrology*, v. 43, no. 1, p. 45–83, <https://doi.org/10.1093/petrology/43.1.45>.

Bhowmik, S.K., Wilde, S.A., Bhandari, A., Pal, T., and Pant, N.C., 2012, Growth of the Greater Indian Landmass and its assembly in Rodinia: Geochronological evidence from the Central Indian Tectonic Zone: *Gondwana Research*, v. 22, no. 1, p. 54–72, <https://doi.org/10.1016/j.gr.2011.09.008>.

Bureau of Geology and Mineral Resources of Sichuan Province (BGMRS), 1980, The Geological map of the People's Republic of China, Yidun Regional: BGMRS Map H-47-16, scale 1: 200,000.

Bureau of Geology and Mineral Resources of Sichuan Province (BGMRS), 1984, The Geological map of the People's Republic of China, Gongling Regional: BGMRS Map H-47-35, scale 1:200,000.

Cawood, P.A., Hawkesworth, C., and Dhuime, B., 2012, Detrital zircon record and tectonic setting: *Geology*, v. 40, p. 875–878, <https://doi.org/10.1130/G32945.1>.

Cawood, P.A., Wang, Y.J., Xu, Y.J., and Zhao, G.C., 2013, Locating South China in Rodinia and Gondwana: A fragment of greater India lithosphere?: *Geology*, v. 41, no. 8, p. 903–906, <https://doi.org/10.1130/G34395.1>.

Cawood, P.A., Zhao, G.C., Yao, J.L., Wang, W., Xu, Y.J., and Wang, Y.J., 2018, Reconstructing South China in Phanerozoic and Precambrian supercontinents: *Earth-Science Reviews*, v. 186, p. 173–194, <https://doi.org/10.1016/j.earscirev.2017.06.001>.

- Chen, Q., Sun, M., Long, X., Zhao, G., and Yuan, C., 2016, U-Pb ages and Hf isotopic record of zircons from the late Neoproterozoic and Silurian–Devonian sedimentary rocks of the western Yangtze block: Implications for its tectonic evolution and continental affinity: *Gondwana Research*, v. 31, p. 184–199, <https://doi.org/10.1016/j.gr.2015.01.009>.
- Chen, Q., Sun, M., Long, X., Zhao, G., Wang, J., Yu, Y., and Yuan, C., 2018, Provenance study for the Paleozoic sedimentary rocks from the west Yangtze block: Constraint on possible link of South China to the Gondwana supercontinent reconstruction: *Precambrian Research*, v. 309, p. 271–289, <https://doi.org/10.1016/j.precamres.2017.01.022>.
- Chen, Q., Zhao, G., and Sun, M., 2021, Protracted northward drifting of South China during the assembly of Gondwana: Constraints from the spatial-temporal provenance comparison of Neoproterozoic–Cambrian strata: *Geological Society of America Bulletin*, v. 133, p. 1947–1963, <https://doi.org/10.1130/B35791.1>.
- Cui, X., Zhu, W.B., Fitzsimons, I.C.W., He, J.W., Lu, Y.Z., Wang, X., Ge, R.F., Zheng, B.H., and Wu, X.H., 2015, U-Pb age and Hf isotope composition of detrital zircons from Neoproterozoic sedimentary units in southern Anhui Province, South China: Implications for the provenance, tectonic evolution and glacial history of the eastern Jiangnan orogen: *Precambrian Research*, v. 271, p. 65–82, <https://doi.org/10.1016/j.precamres.2015.10.004>.
- DeCelles, P.G., Gehrels, G.E., Quade, J., Lareau, B., and Spurlin, M., 2000, Tectonic implications of U-Pb zircon ages of the Himalayan orogenic belt in Nepal: *Science*, v. 288, p. 5465, p. 497–499, <https://doi.org/10.1126/science.288.5465.497>.
- Deng, Q., Wang, Z., Jian, W., Hu, Z., and Fei, Y., 2016, 800–780 Ma continental rift magmatism in the eastern part of the Jiangnan orogen: Implications from ~790 Ma aluminous A-type granites in Zhejiang-Anhui-Jiangxi border area: *Geological Bulletin of China*, v. 35, no. 11, p. 1855–1868.
- Dickinson, W.R., and Gehrels, G.E., 2009, Use of U-Pb ages of detrital zircons to infer maximum depositional ages of strata: A test against a Colorado Plateau Mesozoic database: *Earth and Planetary Science Letters*, v. 288, no. 1–2, p. 115–125, <https://doi.org/10.1016/j.epsl.2009.09.013>.
- Du, Q.L., 1986, The discovery and subdivision of Precambrian in Shuiluo area, Muli county, Sichuan province [in Chinese with English abstract]: *Journal Chengdu College of Geology*, v. 13, no. 1, p. 31–49.
- Fan, W.M., Wang, Y.J., Zhang, Y.H., Zhang, Y.Z., Jourdan, F., and Liu, H.C., 2015, Paleotectonic subduction process revealed from Triassic blueschists in the Lancang tectonic belt of Southwest China: *Tectonophysics*, v. 662, p. 95–108, <https://doi.org/10.1016/j.tecto.2014.12.021>.
- Faure, M., Nguyen, V.V., Hoai, L.T.T., and Lepvrier, C., 2018, Early Paleozoic or Early–Middle Triassic collision between the South China and Indochina blocks: The controversy resolved? Structural insights from the Kon Tum massif (Central Vietnam): *Journal of Asian Earth Sciences*, v. 166, p. 162–180, <https://doi.org/10.1016/j.jseas.2018.07.015>.
- Gardner, C.J., Graham, I.T., Belousova, E., Booth, G.W., and Greig, A., 2017, Evidence for Ordovician subduction-related magmatism in the Truong Son terrane, SE Laos: Implications for Gondwana evolution and porphyry Cu exploration potential in SE Asia: *Gondwana Research*, v. 44, p. 139–156, <https://doi.org/10.1016/j.gr.2016.11.003>.
- Gehrels, G.E., Decelles, P.G., Ojha, T.P., and Upreti, B.N., 2006, Geologic and U-Pb geochronologic evidence for early Paleozoic tectonism in the Dadeladhura thrust sheet, far-west Nepal Himalaya: *Journal of Asian Earth Sciences*, v. 28, no. 4–6, p. 385–408, <https://doi.org/10.1016/j.jseas.2005.09.012>.
- Gehrels, G., Kapp, P., DeCelles, P., Pullen, A., Blakey, R., Weislogel, A., Ding, L., Gynn, J., Martin, A., McQuarrie, N., and Yin, A., 2011, Detrital zircon geochronology of pre-tertiary strata in the Tibetan-Himalayan orogen: *Tectonics*, v. 30, no. 5, p. 1–27, <https://doi.org/10.1029/2011TC002868>.
- Gregory, L.C., Meert, J.G., Bingen, B., Pandit, M.K., and Torsvik, T.H., 2009, Paleomagnetism and geochronology of the Malani igneous suite, northwest India: Implications for the configuration of Rodinia and the assembly of Gondwana: *Precambrian Research*, v. 170, no. 1–2, p. 13–26, <https://doi.org/10.1016/j.precamres.2008.11.004>.
- Haines, P.W., Kirkland, C.L., Wingate, M.T.D., Allen, H., Belousova, E.A., and Gréau, Y., 2016, Tracking sediment dispersal during orogenesis: A zircon age and Hf isotope study from the western Amadeus basin, Australia: *Gondwana Research*, v. 37, p. 324–347, <https://doi.org/10.1016/j.gr.2015.08.011>.
- Handke, M.J., Tucker, R.D., and Ashwal, L.D., 1999, Neoproterozoic continental arc magmatism in west-central Madagascar: *Geology*, v. 27, no. 4, p. 351–354, [https://doi.org/10.1130/0091-7613\(1999\)027<0351:NCAMIW>2.3.CO;2](https://doi.org/10.1130/0091-7613(1999)027<0351:NCAMIW>2.3.CO;2).
- Harris, C., and Ashwal, L.D., 2002, The origin of low $\delta^{18}\text{O}$ granites and related rocks from the Seychelles: Contributions to Mineralogy and Petrology, v. 143, no. 3, p. 366–376, <https://doi.org/10.1007/s00410-002-0349-6>.
- He, Y.Y., Niu, Z.J., Yao, H.Z., Song, F., and Yang, W.Q., 2020, Provenance and tectonic setting of the Ordovician sedimentary succession at the southeastern margin of the Yangtze block, South China: Implications for paleotopographic evolution of northeastern Gondwana: *Journal of Asian Earth Sciences*, v. 202, <https://doi.org/10.1016/j.jseas.2020.104532>.
- Hofmann, M., Linnemann, U., Rai, V., Becker, S., Gartner, A., and Sagawe, A., 2011, The India and South China cratons at the margin of Rodinia—synchronous Neoproterozoic magmatism revealed by LA-ICP-MS zircon analyses: *Lithos*, v. 123, no. 1–4, p. 176–187, <https://doi.org/10.1016/j.lithos.2011.01.012>.
- Hofmann, M.H., Li, X.H., Chen, J., MacKenzie, L.A., and Hinman, N.W., 2016, Provenance and temporal constraints of the Early Cambrian Maotianshan shale, Yunnan province, China: *Gondwana Research*, v. 37, p. 348–361, <https://doi.org/10.1016/j.gr.2015.08.015>.
- Hou, Z.Q., Qu, X.M., Zhou, J.R., Yang, Y.Q., Huang, D.H., Lv, Q.T., Tang, S.H., Yu, J.J., Wang, H.P., and Zhao, J.H., 2001, Collision-orogenic processes of the Yidun arc in the Sanjiang region: Record of granites [in Chinese with English abstract]: *Acta Geologica Sinica*, v. 75, no. 4, p. 484–497.
- Hou, Z.Q., Yang, Y.Q., Wang, H.P., Qu, X.M., Lv, Q.T., Huang, D.H., Wu, X.Z., Yu, J.J., Tang, S.H., and Zhao, J.H., 2004, Tectonic evolution and mineralization systems of the Yidun Arc orogen in Sanjiang Region, China [in Chinese with English abstract]: *Acta Geologica Sinica*, v. 78, no. 1, p. 109–120.
- Hu, P.Y., Li, C., Wu, Y.W., Xie, C.M., Wang, M., Zhang, H.Y., and Li, J., 2014, The Silurian Tethyan Ocean in central Qiangtang, northern Tibet: Constraints from zircon U-Pb ages of plagiogranites within the Taoxinghu ophiolite: *Geological Bulletin of China*, v. 33, no. 11, p. 1651–1661.
- Huang, D.L., Wang, X.L., Xia, X.P., Wan, Y.S., Zhang, F.F., Li, J.Y., and Du, D.H., 2018, Neoproterozoic low- $\delta^{18}\text{O}$ zircons revisited: Implications for Rodinia configuration: *Geophysical Research Letters*, v. 46, no. 2, p. 678–688, <https://doi.org/10.1029/2018GL081117>.
- Hughes, N.C., Myrow, P.M., McKenzie, N.R., Harper, D.A.T., Bhargava, O.N., Tangri, S.K., Ghalley, K.S., and Fanning, C.M., 2011, Cambrian rocks and faunas of the Wachi La, Black Mountains, Bhutan: *Geological Magazine*, v. 148, no. 3, p. 351–379, <https://doi.org/10.1017/S0016756810000750>.
- Hughes, N.C., Myrow, P.M., Ghazi, S., McKenzie, N.R., Stockli, D.F., and DiPietro, J.A., 2019, Cambrian geology of the Salt Range of Pakistan: Linking the Himalayan margin to the Indian craton: *Geological Society of America Bulletin*, v. 131, no. 7–8, p. 1095–1114, <https://doi.org/10.1130/B35092.1>.
- Jian, P., Liu, D.Y., Kröner, A., Zhang, Q., Wang, Y.Z., Sun, X.M., and Zhang, W., 2009, Devonian to Permian plate tectonic cycle of the Paleo-Tethys orogen in southwest China: Insights from zircon ages of ophiolites, arc/back-arc assemblages and within-plate igneous rocks and generation of the Emeishan CFB province: *Lithos*, v. 113, p. 767–784, <https://doi.org/10.1016/j.lithos.2009.04.006>.
- Jiang, G.Q., Sohl, L.E., and Christie-Blick, N., 2003, Neoproterozoic stratigraphic comparison of the Lesser Himalaya (India) and Yangtze block (South China): Paleogeographic implications: *Geology*, v. 31, no. 10, p. 917–920, <https://doi.org/10.1130/G19790.1>.
- Jiang, X.W., Zou, H., Bagas, L., Chen, H.F., Liu, H., Li, Y., Li, M., and Li, D., 2020, The Mojiawan I-type granite of the Kangding Complex in the western Yangtze block: New constraint on the Neoproterozoic magmatism and tectonic evolution of South China: *International Geology Review*, v. 63, p. 2293–2313, <https://doi.org/10.1080/00206814.2020.1833254>.
- Johnson, E.L., Phillips, G., and Allen, C.M., 2016, Ediacaran–Cambrian basin evolution in the Koonenberry Belt (eastern Australia): Implications for the geodynamics of the Delamerian orogen: *Gondwana Research*, v. 37, p. 266–284, <https://doi.org/10.1016/j.gr.2016.04.010>.
- Keeman, J., Turner, S., Haines, W.P., Belousova, E., Ireland, T., Brouwer, P., Fodend, J., and Wörner, G., 2020, New U-Pb, Hf and O isotope constraints on the provenance of sediments from the Adelaide Rift Complex—Documenting the key Neoproterozoic to Early Cambrian succession: *Gondwana Research*, v. 83, p. 248–278, <https://doi.org/10.1016/j.gr.2020.02.005>.
- Kröner, A., Hegner, E., Collins, A.S., Windley, B.F., Brewer, T.S., Razakamanana, T., and Pidgeon, R.T., 2000, Age and magmatic history of the Antananarivo block, central Madagascar, as derived from zircon geochronology and Nd isotopic systematics: *American Journal of Science*, v. 300, no. 4, p. 251–288, <https://doi.org/10.2475/ajsl.300.4.251>.
- Lan, Z.W., Zhang, S.J., Li, X.H., Pandey, S.K., Sharma, M., Shukla, Y., Ahmad, S., Sarkar, S., and Zhai, M.G., 2020, Towards resolving the ‘jigsaw puzzle’ and age-fossil inconsistency within East Gondwana: *Precambrian Research*, v. 345, p. 1–18, <https://doi.org/10.1016/j.precamres.2020.105775>.
- Li, X.H., Long, W.G., Li, Q.L., Liu, Y., Zheng, Y.F., Yang, Y.H., Chamberlain, K.R., Wan, D.F., Guo, C.H., Wang, X.C., and Tao, H., 2010, Penglai zircon megacrysts: A potential new working reference material for microbeam determination of Hf–O isotopes and U–Pb age: *Geostandards and Geoanalytical Research*, v. 34, no. 2, p. 117–134, <https://doi.org/10.1111/j.1751-908X.2010.00036.x>.
- Li, J.Y., Wang, X.L., and Gu, Z.D., 2018, Petrogenesis of the Jiaoziding granitoids and associated basaltic porphyries: Implications for extensive early Neoproterozoic arc magmatism in western Yangtze block: *Lithos*, v. 296, p. 547–562, <https://doi.org/10.1016/j.lithos.2017.11.034>.
- Li, X.H., Li, Z.X., Zhou, H.W., Liu, Y., and Kinny, P.D., 2002, U-Pb zircon geochronology, geochemistry and Nd isotopic study of Neoproterozoic bimodal volcanic rocks in the Kangdian Rift of South China: Implications for the initial rifting of Rodinia: *Precambrian Research*, v. 113, no. 1–2, p. 135–154, [https://doi.org/10.1016/S0301-9268\(01\)00207-8](https://doi.org/10.1016/S0301-9268(01)00207-8).
- Li, X.H., Li, W.X., Li, Z.X., and Liu, Y., 2008, 850–790 Ma bimodal volcanic and intrusive rocks in northern Zhejiang, South China: A major episode of continental rift magmatism during the breakup of Rodinia: *Lithos*, v. 102, no. 1–2, p. 341–357, <https://doi.org/10.1016/j.lithos.2007.04.007>.
- Li, Y.X., Yin, C.Q., Lin, S.F., Zhang, J., Gao, P., Qian, J.H., Xia, Y.F., and Liu, J.N., 2021, Geochronology and geochemistry of bimodal volcanic rocks from the western Jiangnan orogenic belt: Petrogenesis, source nature and tectonic implication: *Precambrian Research*, v. 359, <https://doi.org/10.1016/j.precamres.2021.106218>.
- Li, Z.X., Li, X.H., Kinny, P.D., and Wang, J., 1999, The breakup of Rodinia: Did it start with a mantle plume beneath South China? *Earth and Planetary Science Letters*, v. 173, no. 3, p. 171–181, [https://doi.org/10.1016/S0012-821X\(99\)00240-X](https://doi.org/10.1016/S0012-821X(99)00240-X).
- Liu, B.B., Peng, T.P., Fan, W.M., Zhao, G.C., Gao, J.F., Dong, X.H., and Peng, B.X., 2020a, Tectonic evolution and paleoexposure of the Baoshan and Lincang blocks of West Yunnan during the Paleozoic: *Tectonics*, v. 39, no. 10, <https://doi.org/10.1029/2019TC006028>.
- Liu, H., Wang, Z.J., Deng, Q., Du, Q.D., and Yang, F., 2019a, Constraints on the onset age of the Sturtian glaciation

- from the Southeast Yangtze block, South China: *International Geology Review*, v. 61, no. 15, p. 1876–1886, <https://doi.org/10.1080/00206814.2019.1566787>.
- Liu, S.L., Cui, X.Z., Wang, C.L., Ren, G.M., Wang, P., Pang, W.H., and Ren, F., 2020b, New sedimentological and geochronological evidence for Mid-Neoproterozoic rifting in Western Yangtze block, South China [in Chinese with English abstract]: *Earth Science*, v. 45, no. 8, p. 3082–3093, <https://doi.org/10.3799/dqkx.2020.145>.
- Liu, X.J., Xu, Z.Q., Zhen, Y.L., and Ma, Z.L., 2019c, Characteristics of detrital zircon U-Pb geochronology and Hf isotopes from Liwu Group within the Changqiang dome on the southeastern margin of Songpan–Ganzi terrane and its tectonic implications [in Chinese with English abstract]: *Acta Petrologica Sinica (Yanshi Xuebao)*, v. 35, no. 6, p. 169–1716, <https://doi.org/10.18654/1000-0569/2019.06.05>.
- Liu, Y., Yang, K.G., Polat, A., and Ma, X., 2019b, Reconstruction of the Cryogenian palaeogeography in the Yangtze Domain: Constraints from detrital age patterns: *Geological Magazine*, v. 156, no. 7, p. 1247–1264, <https://doi.org/10.1017/S0016756818000535>.
- Liu, Y.S., Hu, Z.C., Zong, K.Q., Gao, C.G., Gao, S., Xu, J., and Chen, H.H., 2010, Reappraisal and refinement of zircon U-Pb isotope and trace element analyses by LA-ICP-MS: *Chinese Science Bulletin*, v. 55, no. 15, p. 1535–1546, <https://doi.org/10.1007/s11434-010-3052-4>.
- Long, S., McQuarrie, N., Tobgay, T., Rose, C., Gehrels, G., and Grujic, D., 2011, Tectonostratigraphy of the lesser Himalaya of Bhutan: Implications for the along-strike stratigraphic continuity of the northern Indian margin: *Geological Society of America Bulletin*, v. 123, no. 7–8, p. 1406–1426, <https://doi.org/10.1130/B30202.1>.
- Ludwig, K.R., 2003, *User's Manual for Isoplot 3.00: A Geochronological Toolkit for Microsoft Excel*: Berkeley, California, USA, Berkeley Geochronology Center Special Publication 4, 74 p.
- Luo, B.J., et al., 2018, Neoproterozoic continental back-arc rift development in the Northwestern Yangtze block: Evidence from the Hannan intrusive magmatism: *Gondwana Research*, v. 59, p. 27–42, <https://doi.org/10.1016/j.gr.2018.03.012>.
- Luo, L., Zeng, L.B., Wang, K., Yu, X.X., Li, Y.H., Zhu, C.X., and Liu, S.N., 2020, Provenance investigation for the Cambrian–Ordovician strata from the northern margin of the western Yangtze block: Implications for locating the South China block in Gondwana: *Geological Magazine*, v. 157, no. 4, p. 551–572, <https://doi.org/10.1017/S0016756819001110>.
- Ma, X., Yang, K.G., and Polat, A., 2019, U-Pb ages and Hf isotopes of detrital zircons from pre-Devonian sequences along the southeast Yangtze: A link to the final assembly of East Gondwana: *Geological Magazine*, v. 156, no. 6, p. 950–968, <https://doi.org/10.1017/S0016756818000511>.
- Malone, S.J., Meert, J.G., Banerjee, D.M., Pandit, M.K., Tamrat, E., Kamenov, G.D., Pradhan, V.R., and Sohl, L.E., 2008, Paleomagnetism and detrital zircon geochronology of the upper Vindhyan Sequence, Son Valley and Rajasthan, India: A ca. 1000 Ma closure age for the Purana basins: *Precambrian Research*, v. 164, no. 3–4, p. 137–159, <https://doi.org/10.1016/j.precamres.2008.04.004>.
- McKenzie, N.C., Hughes, P.M., Myrow, P.M., Banerjee, D.M., Deb, M., and Planavsky, N.J., 2013, New age constraints for the Proterozoic Aravalli-Delhi successions of India and their implications: *Precambrian Research*, v. 238, p. 120–128, <https://doi.org/10.1016/j.precamres.2013.10.006>.
- McKenzie, N.R., Hughes, N.C., Myrow, P.M., Xiao, S., and Sharma, M., 2011, Correlation of Precambrian–Cambrian sedimentary successions across northern India and the utility of isotopic signatures of Himalayan lithotectonic zones: *Earth and Planetary Science Letters*, v. 312, no. 3–4, p. 471–483, <https://doi.org/10.1016/j.epsl.2011.10.027>.
- McQuarrie, N., Long, S.P., Tobgay, T., Nesbit, J.N., Gehrels, G., and Ducea, M.N., 2013, Documenting basin scale, geometry and provenance through detrital geochemical data: Lessons from the Neoproterozoic to Ordovician lesser, greater, and Tethyan Himalayan strata of Bhutan: *Gondwana Research*, v. 23, no. 4, p. 1491–1510, <https://doi.org/10.1016/j.gr.2012.09.002>.
- Metcalfe, I., 2013, Gondwana dispersion and Asian accretion: Tectonic and palaeogeographic evolution of eastern Tethys: *Journal of Asian Earth Sciences*, v. 66, p. 1–33, <https://doi.org/10.1016/j.jseaes.2012.12.020>.
- Mukherjee, P.K., Jain, A.K., Singhal, S., Singha, N.B., Singh, S., Kumud, K., Seth, P., and Patel, R.C., 2019, U-Pb zircon ages and Sm-Nd isotopic characteristics of the lesser and great Himalayan sequences, Uttarakhand Himalaya, and their regional tectonic implications: *Gondwana Research*, v. 75, p. 282–297, <https://doi.org/10.1016/j.gr.2019.06.001>.
- Mulder, J.A., Everard, J.L., Cumming, G., Meffre, S., Bottrill, R.S., Meredith, A.S., Halpin, J.A., McNeill, A.W., and Cawood, P.A., 2020, Neoproterozoic opening of the Pacific Ocean recorded by multi-stage rifting in Tasmania, Australia: *Earth-Science Reviews*, v. 201, p. 1–29, <https://doi.org/10.1016/j.earscirev.2019.103041>.
- Myrow, P.M., Hughes, N.C., Goodge, J.W., Fanning, C.M., Williams, I.S., and Peng, S., 2010, Extraordinary transport and mixing of sediment across Himalayan central Gondwana during the Cambrian–Ordovician: *Geological Society of America Bulletin*, v. 122, no. 9–10, p. 1660–1670, <https://doi.org/10.1130/B30123.1>.
- Nakajima, T., 2013, Late Cenozoic tectonic events and intracarc basin development in Northeast Japan, *in* Itoh, Y., ed., *Mechanism of sedimentary basin formation—multi-disciplinary approach on active plate margins*: Rijeka, Croatia, Tech. p. 153–189, DOI: <https://doi.org/10.5772/57676>.
- Nédélec, A., Paquette, J.L., Antonio, P., Paris, G., and Bouchet, J.L., 2016, A-type stratoid granites of Madagascar revisited: Age, source and links with the breakup of Rodinia: *Precambrian Research*, v. 280, p. 231–248, <https://doi.org/10.1016/j.precamres.2016.04.013>.
- Nguyen, Q.M., Feng, Q., Zi, J.W., Zhao, T., Tran, H.T., Ngo, T.X., Tran, D.M., and Nguyen, H.Q., 2019, Cambrian intra-oceanic arc trondhjemite and tonalite in the Tam Ky-Phuoc Son suture zone, central Vietnam: Implications for the early Paleozoic assembly of the Indochina block: *Gondwana Research*, v. 70, p. 151–170, <https://doi.org/10.1016/j.gr.2019.01.002>.
- Pan, G.T., Ding, J., Wang, L.Q., and Yao, D.S., 2004, Geological map of Qinghai–Xizang (Tibetan) Plateau and adjacent areas [in Chinese with English abstract]: Chengdu, China, Chengdu Cartographic Publishing House, scale 1:1500,000, p. 60–62.
- Peng, T.P., Zhao, G.C., Fan, W.M., Peng, B.X., and Mao, Y.S., 2014, Zircon geochronology and Hf isotopes of Mesozoic intrusive rocks from the Yidun terrane, Eastern Tibetan Plateau: Petrogenesis and their bearings with Cu mineralization: *Journal of Asian Earth Sciences*, v. 80, p. 18–33, <https://doi.org/10.1016/j.jseaes.2013.10.028>.
- Qasim, M., Ding, L., Khan, M.A., Umar, M., Jadoon, I.A.K., Haneef, M., Baral, U., Cai, F.L., Shah, A., and Yao, W., 2018, Late Neoproterozoic–early Palaeozoic stratigraphic succession, western Himalaya, North Pakistan: Detrital zircon provenance and tectonic implications: *Geological Journal*, v. 53, no. 5, p. 2258–2279, <https://doi.org/10.1002/gj.3063>.
- Qi, H., and Zhao, J.H., 2020, Petrogenesis of the Neoproterozoic low- $\delta^{18}\text{O}$ granitoids at the western margin of the Yangtze block in South China: *Precambrian Research*, v. 351, <https://doi.org/10.1016/j.precamres.2020.105953>.
- Qi, L., Cawood, P.A., Xu, Y.J., Du, Y.S., Zhang, H.C., and Zhang, Z.K., 2020, Linking South China to North India from the late Tonian to Ediacaran: Constraints from the Cathaysia block: *Precambrian Research*, v. 350, <https://doi.org/10.1016/j.precamres.2020.105898>.
- Qi, L., Xu, Y.J., Cawood, P.A., and Du, Y.S., 2018, Reconstructing Cryogenian to Ediacaran successions and paleogeography of the South China block: *Precambrian Research*, v. 314, p. 452–467, <https://doi.org/10.1016/j.precamres.2018.07.003>.
- Reid, A., Wilson, C.J., Shun, L., Pearson, N., and Belousova, E., 2007, Mesozoic plutons of the Yidun Arc, SW China: U/Pb geochronology and Hf isotopic signature: *Ore Geology Reviews*, v. 31, no. 1–4, p. 88–106, <https://doi.org/10.1016/j.oregeorev.2004.11.003>.
- Shellnutt, J.G., Nguyen, D.T., and Lee, H.Y., 2020, Resolving the origin of the Seychelles microcontinent: Insight from zircon geochronology and Hf isotopes: *Precambrian Research*, v. 343, <https://doi.org/10.1016/j.precamres.2020.105725>.
- Sowerbutts, A., 2000, Sedimentation and volcanism linked to multiphase rifting in an Oligo–Miocene intracarc basin, Anglona, Sardinia: *Geological Magazine*, v. 137, no. 4, p. 395–418, <https://doi.org/10.1017/S0016756800004246>.
- Sun, J.J., Shu, L.S., Santosh, M., and Wang, L.S., 2018, Precambrian crustal evolution of the central Jiangnan orogen (South China): Evidence from detrital zircon U-Pb ages and Hf isotopic compositions of Neoproterozoic metasedimentary rocks: *Precambrian Research*, v. 318, p. 1–24, <https://doi.org/10.1016/j.precamres.2018.09.008>.
- Sun, W.H., Zhou, M.F., Yan, D.P., Li, J.W., and Ma, Y.X., 2008, Provenance and tectonic setting of the Neoproterozoic Yanbian Group, western Yangtze block (SW China): *Precambrian Research*, v. 167, no. 1, p. 213–236, <https://doi.org/10.1016/j.precamres.2008.08.001>.
- Sun, W.H., Zhou, M.F., Gao, J.F., Yang, Y.H., Zhao, X.F., and Zhao, J.H., 2009, Detrital zircon U-Pb geochronological and Lu–Hf isotopic constraints on the Precambrian magmatic and crustal evolution of the western Yangtze block, SW China: *Precambrian Research*, v. 172, no. 1–2, p. 99–126, <https://doi.org/10.1016/j.precamres.2009.03.010>.
- Tian, Z.D., Leng, C.B., Zhang, X.C., Yin, C.J., Zhang, W., Guo, J.H., and Chen, L.H., 2018, Mineralogical and petrogeochemical characteristics of the metamorphic basement of Yidun terrane and their geological implications [in Chinese with English abstract]: *Acta Mineralogica Sinica*, v. 38, no. 2, p. 152–165, <https://doi.org/10.16461/j.cnki.1000-4734.2018.02.1>.
- Tian, Z.D., Leng, C.B., and Zhang, X.C., 2020, Provenance and tectonic setting of the Neoproterozoic meta-sedimentary rocks at southeastern Tibetan Plateau: Implications for the tectonic affinity of Yidun terrane: *Precambrian Research*, v. 344, p. 1–19, <https://doi.org/10.1016/j.precamres.2020.105736>.
- Tucker, R.D., Ashwal, L.D., Hamilton, M.A., Torsvik, T.H., and Carter, L.M., 1999, Neoproterozoic silicic magmatism of northern Madagascar, Seychelles, and NW India: clues to Rodinia's assembly and dispersal, in *Proceedings: Geological Society of America Abstracts with Programs*, v. 31, no. 7, p. 317.
- Turner, C.C., Meert, J.G., Pandit, M.K., and Kamenov, G.D., 2014, A detrital zircon U-Pb and Hf isotopic transect across the Son Valley sector of the Vindhyan basin, India: Implications for basin evolution and paleogeography: *Gondwana Research*, v. 26, no. 1, p. 348–364, <https://doi.org/10.1016/j.gr.2013.07.009>.
- Valley, J.W., Kinny, P.D., Schulze, D.J., and Spicuzza, M.J., 1998, Zircon megacrysts from kimberlite: Oxygen isotope variability among mantle melts: Contributions to Mineralogy and Petrology, v. 133, no. 1, p. 1–11, <https://doi.org/10.1007/s0041000050432>.
- Verdel, C., Campbell, M.J., and Allen, C.M., 2021, Detrital zircon petrochronology of central Australia, and implications for the secular record of zircon trace element composition: *Geosphere*, v. 17, no. 2, p. 538–560, <https://doi.org/10.1130/GES02300.1>.
- Wang, B.Q., Zhou, M.F., Chen, W.T., Gao, J.F., and Yan, D.P., 2013a, Petrogenesis and tectonic implications of the Triassic volcanic rocks in the northern Yidun terrane, Eastern Tibet: *Lithos*, v. 175, p. 285–301, <https://doi.org/10.1016/j.lithos.2013.05.013>.
- Wang, J., and Li, Z.X., 2003, History of Neoproterozoic rift basins in South China: Implications for Rodinia breakup: *Precambrian Research*, v. 122, no. 1–4, p. 141–158, [https://doi.org/10.1016/S0301-9268\(02\)00209-7](https://doi.org/10.1016/S0301-9268(02)00209-7).
- Wang, J.Q., Shu, L.S., Santosh, M., and Xu, Z.Q., 2015, The pre-Mesozoic crustal evolution of the Cathaysia block, South China: Insights from geological investigation, zircon U-Pb geochronology, Hf isotope and REE geochemistry from the Wugongshan complex: *Gondwana Research*, v. 28, no. 1, p. 225–245, <https://doi.org/10.1016/j.gr.2014.03.008>.
- Wang, W., Cawood, P.A., Zhou, M.F., Pandit, M.K., Xia, X.P., and Zhao, J.H., 2017a, Low- $\delta^{18}\text{O}$ rhyolites from

- the Malani Igneous Suite: A positive test for South China and NW India linkage in Rodinia: *Geophysical Research Letters*, v. 44, no. 20, p. 10,298–10,305, <https://doi.org/10.1002/2017GL074717>.
- Wang, J.Q., Shu, L.S., and Santosh, M., 2017b, U-Pb and Lu-Hf isotopes of detrital zircon grains from Neoproterozoic sedimentary rocks in the central Jiangnan orogen, South China: Implications for Precambrian crustal evolution: *Precambrian Research*, v. 294, p. 175–188, <https://doi.org/10.1016/j.precamres.2017.03.025>.
- Wang, K.X., Sun, L.Q., Sun, T., Huang, H., and Qin, L.S., 2018c, Provenance, weathering conditions, and tectonic evolution history of the Cambrian meta-sediments in the Zhuguangshan area, Cathaysia block: *Precambrian Research*, v. 311, p. 195–210, <https://doi.org/10.1016/j.precamres.2018.04.011>.
- Wang, L.J., Yu, J.H., Griffin, W.L., and O'Reilly, S.Y., 2012a, Early crustal evolution in the western Yangtze block: Evidence from U-Pb and Lu-Hf isotopes on detrital zircons from sedimentary rocks: *Precambrian Research*, v. 222–223, p. 368–385, <https://doi.org/10.1016/j.precamres.2011.08.001>.
- Wang, P.M., Yu, J.H., Sun, T., Ling, H.F., Chen, P.R., Zhao, K.D., Chen, W.F., and Liu, Q., 2012b, Geochemistry and detrital zircon geochronology of Neoproterozoic sedimentary rocks in eastern Hunan Province and their tectonic significance [in Chinese with English abstract]: *Acta Petrologica Sinica (Yanshi Xuebao)*, v. 28, no. 12, p. 3841–3857.
- Wang, P.M., Yu, J.H., Sun, T., Shi, Y., Chen, P.R., Zhao, K.D., Chen, W.F., and Liu, Q., 2013b, Composition variations of the Sinian–Cambrian sedimentary rocks in Hunan and Guangxi provinces and their tectonic significance: *Science China Earth Sciences*, v. 56, no. 11, p. 1899–1917, <https://doi.org/10.1007/s11430-013-4634-1>.
- Wang, Q.F., Deng, J., Li, C.S., Li, G.J., Li, Y., and Qiao, L., 2014, The boundary between the Simao and Yangtze blocks and their locations in Gondwana and Rodinia: Constraints from detrital and inherited zircons: *Gondwana Research*, v. 26, no. 2, p. 438–448, <https://doi.org/10.1016/j.gr.2013.10.002>.
- Wang, W., Zeng, M.F., Zhou, M.F., Zhao, J.H., Zheng, J.P., and Lan, Z.F., 2018b, Age, provenance and tectonic setting of Neoproterozoic to early Paleozoic sequences in southeastern South China block: Constraints on its linkage to western Australia-east Antarctica: *Precambrian Research*, v. 309, p. 290–308, <https://doi.org/10.1016/j.precamres.2017.03.002>.
- Wang, W., Cawood, P.A., Pandit, M.K., Zhao, J.H., and Zheng, J.P., 2019a, No collision between Eastern and Western Gondwana at their northern extent: *Geology*, v. 47, no. 4, p. 308–312, <https://doi.org/10.1130/G45745.1>.
- Wang, W., Cawood, P.A., Pandit, M.K., Xia, X.P., Raveggi, M., Zhao, J.H., Zheng, J.P., and Qi, L., 2021, Fragmentation of South China from greater India during the Rodinia-Gondwana transition: *Geology*, v. 49, no. 2, p. 228–232, <https://doi.org/10.1130/G48308.1>.
- Wang, X.C., Li, X.H., Li, W.X., and Li, Z.X., 2007a, Ca. 825 Ma komatiitic basalts in South China: First evidence for >1500 °C mantle melts by a Rodinian mantle plume: *Geology*, v. 35, no. 12, p. 1103–1106, <https://doi.org/10.1130/G23878A.1>.
- Wang, X.C., Li, Z.X., Li, X.H., Li, Q.L., Tang, G.Q., Zhang, Q.R., and Liu, Y., 2011, Nonglacial origin for low-delta $\delta^{18}\text{O}$ Neoproterozoic magmas in the South China block: Evidence from new in-situ oxygen isotope analyses using SIMS: *Geology*, v. 39, no. 8, p. 735–738, <https://doi.org/10.1130/G31991.1>.
- Wang, X.C., Li, X.H., Li, Z.X., Li, Q.L., Tang, G.Q., Gao, Y.Y., Zhang, Q.R., and Liu, Y., 2012c, Episodic Precambrian crust growth: Evidence from U-Pb ages and Hf-O isotopes of zircon in the Nanhua basin, central South China: *Precambrian Research*, v. 222, p. 386–403, <https://doi.org/10.1016/j.precamres.2011.06.001>.
- Wang, X.L., Zhou, J.C., Griffin, W.L., Wang, R.C., Qiu, J.S., Reilly, S.Y.O., Xu, X.S., Liu, X.M., and Zhang, G.L., 2007b, Detrital zircon geochronology of Precambrian basement sequences in the Jiangnan orogen: Dating the assembly of the Yangtze and Cathaysia blocks: *Precambrian Research*, v. 159, no. 1–2, p. 117–131, <https://doi.org/10.1016/j.precamres.2007.06.005>.
- Wang, X.L., Zhou, J.C., Wan, Y.S., Kitajima, K., Wang, D., Bonamici, C., Qiu, J.S., and Sun, T., 2013c, Magmatic evolution and crustal recycling for Neoproterozoic strongly peraluminous granitoids from southern China: Hf and O isotopes in zircon: *Earth and Planetary Science Letters*, v. 366, p. 71–82, <https://doi.org/10.1016/j.epsl.2013.02.011>.
- Wang, Y.J., Zhang, F.F., Fan, W.M., Zhang, G.W., Chen, S.Y., Cawood, P.A., and Zhang, A.M., 2010, Tectonic setting of the South China block in the early Paleozoic: Resolving intracontinental and ocean closure models from detrital zircon U-Pb geochronology: *Tectonics*, v. 29, no. 6, p. 1–16, <https://doi.org/10.1029/2010TC002750>.
- Wang, Z.H., Yang, W.Q., Zhou, D., Niu, Z.J., He, Y.Y., and Song, F., 2018a, Detrital zircon U-Pb geochronological records and its response of provenance transformation of strata surrounding Cambrian–Devonian unconformity in eastern margin of Yunkai Massif [in Chinese with English abstract]: *Earth Science*, v. 43, no. 11, p. 4193–4203, <https://doi.org/10.3799/dqkx.2018.242>.
- Wu, L., Jia, D., Li, H.B., Deng, F., and Li, Y.Q., 2010, Provenance of detrital zircons from the late Neoproterozoic to Ordovician sandstones of South China: Implications for its continental affinity: *Geological Magazine*, v. 147, no. 6, p. 974–980, <https://doi.org/10.1017/S0016756810000725>.
- Wu, P., Zhang, S.B., Zheng, Y.F., Li, Q.L., Li, Z.X., and Sun, F.Y., 2020, The occurrence of Neoproterozoic low $\delta^{18}\text{O}$ igneous rocks in the northwestern margin of the South China block: Implications for the Rodinia configuration: *Precambrian Research*, v. 347, <https://doi.org/10.1016/j.precamres.2020.105841>.
- Wu, Y.W., 2013, The evolution record of Longmuco–Shuanghu–Lancang Ocean–Cambrian–Permian ophiolites [Ph.D. dissertation]: Changchun, Jilin, China, Jilin University, 238 p. [in Chinese with English abstract].
- Xiang, L., and Shu, L.S., 2010, Pre-Devonian tectonic evolution of the eastern South China block: Geochronological evidence from detrital zircons [in Chinese with English abstract]: *Science China Earth Sciences*, v. 53, no. 10, p. 1427–1444, <https://doi.org/10.1007/s11430-010-4061-5>.
- Xiong, C., Niu, Y.L., Chen, H.D., Chen, A.Q., Zhang, C.G., Li, F., Yang, S., and Xu, S.L., 2019, Detrital zircon U-Pb geochronology and geochemistry of late Neoproterozoic–Early Cambrian sedimentary rocks in the Cathaysia block: Constraint on its palaeo-position in Gondwana supercontinent: *Geological Magazine*, v. 156, no. 9, p. 1587–1604, <https://doi.org/10.1017/S0016756819000013>.
- Xu, Y.J., Cawood, P.A., Du, Y.S., Hu, L.S., Yu, W.C., Zhu, Y.H., and Li, W.C., 2013, Linking South China to northern Australia and India on the margin of Gondwana: Constraints from detrital zircon U-Pb and Hf isotopes in Cambrian strata: *Tectonics*, v. 32, no. 6, p. 1547–1558, <https://doi.org/10.1002/tect.20099>.
- Xu, Y.J., Cawood, P.A., Du, Y.S., Huang, H.W., and Wang, X.Y., 2014, Early Paleozoic orogenesis along Gondwana's northern margin constrained by provenance data from South China: *Tectonophysics*, v. 636, p. 40–51, <https://doi.org/10.1016/j.tecto.2014.08.022>.
- Xue, E.K., Wang, W., Huang, S.F., and Lu, G.M., 2019, Detrital zircon U-Pb-Hf isotopes and whole-rock geochemistry of Neoproterozoic–Cambrian successions in the Cathaysia block of South China: Implications on paleogeographic reconstruction in supercontinent: *Precambrian Research*, v. 331, <https://doi.org/10.1016/j.precamres.2019.105348>.
- Yang, C., Li, X.H., Wang, X.C., and Lan, Z., 2015, Mid-Neoproterozoic angular unconformity in the Yangtze block revisited: Insights from detrital zircon U-Pb age and Hf-O isotopes: *Precambrian Research*, v. 266, p. 165–178, <https://doi.org/10.1016/j.precamres.2015.05.016>.
- Yan, C.L., Shu, L.S., Santosh, M., Yao, J.L., Li, J.Y., and Li, C., 2015, The Precambrian tectonic evolution of the western Jiangnan orogen and western Cathaysia block: Evidence from detrital zircon age spectra and geochemistry of clastic rocks: *Precambrian Research*, v. 268, p. 33–60, <https://doi.org/10.1016/j.precamres.2015.07.002>.
- Yan, C.L., Shu, L.S., Faure, M., Chen, Y., and Huang, R.B., 2019, Time constraints on the closure of the Paleoproterozoic South China Ocean and the Neoproterozoic assembly of the Yangtze and Cathaysia blocks: Insight from new detrital zircon analyses: *Gondwana Research*, v. 73, p. 175–189, <https://doi.org/10.1016/j.gr.2019.03.018>.
- Yang, Y.N., Wang, X.C., Li, Q.L., and Li, X.H., 2016, Integrated in situ U-Pb age and Hf-O analyses of zircon from Suixian Group in northern Yangtze: New insights into the Neoproterozoic low- $\delta^{18}\text{O}$ magmas in the South China block: *Precambrian Research*, v. 273, p. 151–164, <https://doi.org/10.1016/j.precamres.2015.12.008>.
- Yang, Z.Y., Sun, Z.M., Yang, T.S., and Pei, J.L., 2004, A long connection (750–380 Ma) between South China and Australia: Paleomagnetic constraints: *Earth and Planetary Science Letters*, v. 220, p. 423–434, [https://doi.org/10.1016/S0012-821X\(04\)00053-6](https://doi.org/10.1016/S0012-821X(04)00053-6).
- Yang, Z.Y., and Jiang, S.Y., 2019, Detrital zircons in metasedimentary rocks of Mayuan and Mamianshan Group from Cathaysia block in northwestern Fujian province, South China: New constraints on their formation ages and paleogeographic implication: *Precambrian Research*, v. 320, p. 13–30, <https://doi.org/10.1016/j.precamres.2018.10.004>.
- Yao, J.L., Shu, L.S., and Santosh, M., 2011, Detrital zircon U-Pb geochronology, Hf-isotopes and geochemistry—new clues for the Precambrian crustal evolution of Cathaysia block, South China: *Gondwana Research*, v. 20, no. 2–3, p. 553–567, <https://doi.org/10.1016/j.gr.2011.01.005>.
- Yao, J.L., Cawood, P.A., Shu, L.S., and Zhao, G.C., 2019, Jiangnan orogen, South China: A similar to 970–820 Ma Rodinia margin accretionary belt: *Earth Science Reviews*, v. 196, 102872, <https://doi.org/10.1016/j.earscirev.2019.05.016>.
- Yao, W.H., Li, Z.X., Li, W.X., Li, X.H., and Yang, J.H., 2014, From Rodinia to Gondwanaland: A tale of detrital zircon provenance analyses from the southern Nanhua basin, South China: *American Journal of Science*, v. 314, no. 1, p. 278–313, <https://doi.org/10.2475/01.2014.08>.
- Yao, W.H., Li, Z.X., Li, W.X., Su, L., and Yang, J.H., 2015, Detrital provenance evolution of the Ediacaran–Silurian Nanhua Foreland basin, South China: *Gondwana Research*, v. 28, no. 4, p. 1465–1488, <https://doi.org/10.1016/j.gr.2014.10.018>.
- Yu, J.H., Reilly, S.Y.O., Wang, L.J., Griffin, W.L., Zhou, M.F., Zhang, M., and Shu, L.S., 2010, Components and episodic growth of Precambrian crust in the Cathaysia block, South China: Evidence from U-Pb ages and Hf isotopes of zircons in Neoproterozoic sediments: *Precambrian Research*, v. 181, no. 1–4, p. 97–114, <https://doi.org/10.1016/j.precamres.2010.05.016>.
- Yuan, H.L., Gao, S., Liu, X.M., Li, H.M., Günther, D., and Wu, F.Y., 2004, Accurate U-Pb age and trace element determinations of zircon by laser ablation inductively coupled plasma-mass spectrometry: *Geostandards and Geoanalytical Research*, v. 28, no. 3, p. 353–370, <https://doi.org/10.1111/j.1751-908X.2004.tb00755.x>.
- Yuan, H.Y., Zhou, Q., Ding, J., Zhang, H.H., Zhu, L.T., Liang, J., Tang, G.L., and Wang, C.N., 2021a, U-Pb geochronological studies on detrital zircon in Jianglang Group, Western Sichuan Province, China [in Chinese with English abstract]: *Acta Mineralogica Sinica*, v. 390–391, no. 3, p. 296–304 <https://doi.org/10.1016/j.lithos.2021.106108>.
- Yuan, X.Y., Niu, M.L., Cai, Q.R., Wu, Q., Zhu, G., Li, X.C., Sun, Y., and Li, C., 2021b, Bimodal volcanic rocks in the northeastern margin of the Yangtze block: Response to breakup of Rodinia supercontinent: *Lithos*, v. 390, p. 106–108, <https://doi.org/10.1016/j.lithos.2021.106108>.
- Zhang, H., Liu, Y.X., Ding, X.Z., Gao, L.Z., Yang, C., Zhang, J.B., Gong, C.Q., and Liu, H.G., 2020a, Geochronology, geochemistry, whole rock Sr-Nd and zircon Hf-O isotopes of the early Neoproterozoic volcanic rocks in Jiangshan, eastern part of the Jiangnan orogen: Constraints on petrogenesis and tectonic implications: *Acta Geologica Sinica*, v. 94, no. 4, p. 1117–1137, <https://doi.org/10.1111/1755-6724.14561>.
- Zhang, J.B., Ni, J.B., Liu, Y.X., Zhang, H., and Bu, L., 2020b, Ordovician proto-basin in South China and its tectonic implications: Evidence from the detrital zircon U-Pb ages of the Ordovician in Central Hunan, China: *Acta*

- Geologica Sinica, v. 94, no. 6, p. 561–583, <https://doi.org/10.1111/1755-6724.14583>.
- Zhang, J.W., Ye, T.P., Dai, Y.R., Chen, J.S., Zhang, H., Dai, C.G., Yuan, G.H., and Jiang, K.Y., 2019a, Provenance and tectonic setting transition as recorded in the Neoproterozoic strata, western Jiangnan orogen: Implications for South China within Rodinia. *Geoscience Frontiers*, v. 10, no. 5, p. 1823–1839, <https://doi.org/10.1016/j.gsf.2018.10.009>.
- Zhang, X.C., Wang, Y.J., Clift, P.D., Yan, Y., Zhang, Y.Z., and Zhang, L., 2018, Paleozoic tectonic setting and paleogeographic evolution of the Qin-Fang region, southern South China block: Detrital zircon U-Pb geochronological and Hf isotopic constraints. *Geochemistry, Geophysics, Geosystems*, v. 19, no. 10, p. 3962–3979, <https://doi.org/10.1029/2018GC007713>.
- Zhang, X.Z., Dong, Y.S., Li, C., Deng, M.R., Zhang, L., and Xu, W., 2014, Silurian high-pressure granulites from Central Qiangtang, Tibet: constraints on early Paleozoic collision along the northeastern margin of Gondwana. *Earth and Planetary Science Letters*, v. 39, p. 39–51, <https://doi.org/10.1016/j.epsl.2014.08.013>.
- Zhang, Y.L., Jia, X.T., Wang, Z.Q., Wang, K.M., and Chen, M.Y., 2019b, Paleogeography and provenance analysis of Early Cambrian Xiannvong Formation in the Miancangshan area [in Chinese with English abstract]. *Acta Geologica Sinica*, v. 93, no. 11, p. 2904–2920, <https://doi.org/10.19762/j.cnki.dizhixuebao.2019094>.
- Zhao, B.X., Long, X.P., Luo, J., Dong, Y.P., Lan, C.Y., Wang, J.Y., and Wu, B., 2021a, Late Neoproterozoic to early Paleozoic paleogeographic position of the Yangtze block and the change of tectonic setting in its northwestern margin: Evidence from detrital zircon U-Pb ages and Hf isotopes of sedimentary rocks. *Geological Society of America Bulletin*, v. 134, no. 1–2, p. 335–347, <https://doi.org/10.1130/B35980.1>.
- Zhao, G.C., and Cawood, P.A., 1999, Tectonothermal evolution of the Mayuan Assemblage in the Cathaysia block: implications for Neoproterozoic collision-related assembly of the South China craton. *American Journal of Science*, v. 299, no. 4, p. 309–339, <https://doi.org/10.2475/ajs.299.4.309>.
- Zhao, G.C., Wang, Y.J., Huang, B.C., Dong, Y.P., Li, S.Z., Zhang, G.W., and Yu, S., 2018a, Geological reconstructions of the East Asian blocks: From the breakup of Rodinia to the assembly of Pangea. *Earth-Science Reviews*, v. 186, p. 262–286, <https://doi.org/10.1016/j.earscirev.2018.10.003>.
- Zhao, J.H., Zhou, M.F., Yan, D.P., Yang, Y.H., and Sun, M., 2008a, Zircon Lu-Hf isotopic constraints on Neoproterozoic subduction-related crustal growth along the western margin of the Yangtze block, South China. *Precambrian Research*, v. 163, no. 3–4, p. 189–209, <https://doi.org/10.1016/j.precamres.2007.11.003>.
- Zhao, J.H., Zhou, M.F., Zheng, J.P., and Fang, S.M., 2010, Neoproterozoic crustal growth and reworking of the Northwestern Yangtze block: Constraints from the Xixiang dioritic intrusion, South China. *Lithos*, v. 120, no. 3–4, p. 439–452, <https://doi.org/10.1016/j.lithos.2010.09.005>.
- Zhao, J.H., Zhou, M.F., Yan, D.P., Zheng, J.P., and Li, J.W., 2011, Reappraisal of the ages of Neoproterozoic strata in South China: No connection with the Grenvillian orogeny. *Geology*, v. 39, no. 4, p. 299–302, <https://doi.org/10.1130/G31701.1>.
- Zhao, J.H., Asimow, P.D., Zhou, M.F., Zhang, J., Yan, D.P., and Zheng, J.P., 2017, An Andean-type arc system in Rodinia constrained by the Neoproterozoic Shimian ophiolite in South China. *Precambrian Research*, v. 296, p. 93–111, <https://doi.org/10.1016/j.precamres.2017.04.017>.
- Zhao, J.H., Pandit, M.K., Wang, W., and Xia, X.P., 2018b, Neoproterozoic tectonothermal evolution of NW India: Evidence from geochemistry and geochronology of granulites. *Lithos*, v. 316, p. 330–346, <https://doi.org/10.1016/j.lithos.2018.07.020>.
- Zhao, J.H., Li, Q.W., Liu, H., and Wang, W., 2018c, Neoproterozoic magmatism in the western and northern margins of the Yangtze block (South China) controlled by slab subduction and subduction-transform-edge-propagator. *Earth-Science Reviews*, v. 187, p. 1–18, <https://doi.org/10.1016/j.earscirev.2018.10.004>.
- Zhao, J.H., Nebel, O., and Johnson, T.E., 2021b, Formation and evolution of a Neoproterozoic continental magmatic arc. *Journal of Petrology*, v. 62, no. 8, p. 1–53, <https://doi.org/10.1093/petrology/egab029>.
- Zhao, X.F., Zhou, M.F., Li, J.W., and Wu, F.Y., 2008b, Association of Neoproterozoic A- and I-type granites in South China: Implications for generation of A-type granites in a Subduction-related Environment. *Chemical Geology*, v. 257, no. 1–2, p. 1–15, <https://doi.org/10.1016/j.chemgeo.2008.07.018>.
- Zhao, Z.B., Xu, Z.Q., Ma, X.X., Liang, F.H., and Guo, P., 2018d, Neoproterozoic-Early Paleozoic tectonic evolution of the South China Craton: New insights from the polyphase deformation in the southwestern Jiangnan orogen. *Acta Geologica Sinica*, v. 92, no. 5, p. 1700–1727, <https://doi.org/10.1111/1755-6724.13672>.
- Zhou, J.L., Shao, S., Luo, Z.H., Shao, J.B., Wu, D.T., and Rao-salamala, V., 2015a, Geochronology and geochemistry of Cryogenian gabbros from the Ambatondrazaka area, east-central Madagascar: Implications for Madagascar-India correlation and Rodinia paleogeography. *Precambrian Research*, v. 256, p. 256–270, <https://doi.org/10.1016/j.precamres.2014.11.005>.
- Zhou, J.L., 2015b, Tectonic affinity of the Neoproterozoic-aged Imorona-Itsindro Suite in Madagascar and its geological significance [thesis]: Beijing, China, China University of Geosciences [in Chinese with English abstract].
- Zhou, J.L., Li, X.H., Tang, G.Q., Liu, Y., and Tucker, R.D., 2017, New evidence for a continental rift tectonic setting of the Neoproterozoic Imorona-Itsindro Suite (central Madagascar). *Precambrian Research*, v. 306, p. 94–111, <https://doi.org/10.1016/j.precamres.2017.12.029>.
- Zhou, J.L., Li, X.H., Tang, G.Q., Liu, Y., and Tucker, R.D., 2018a, New evidence for a continental rift tectonic setting of the Neoproterozoic Imorona-Itsindro Suite (central Madagascar). *Precambrian Research*, v. 306, p. 94–111, <https://doi.org/10.1016/j.precamres.2017.12.029>.
- Zhou, J.L., Li, X.H., and Tucker, R.D., 2020, New insights into the genesis of Neoproterozoic low- $\delta^{18}\text{O}$ granulites in the Seychelles: Crustal cannibalization within an intra-plate extensional setting. *Science Bulletin*, v. 65, no. 22, p. 1880–1883, <https://doi.org/10.1016/j.scib.2020.07.025>.
- Zhou, M.F., Ma, Y., Yan, D.P., Xia, X., Zhao, J.H., and Sun, M., 2006, The Yanbian terrane (Southern Sichuan Province, SW China): A Neoproterozoic arc assemblage in the western margin of the Yangtze block. *Precambrian Research*, v. 144, no. 1–2, p. 19–38, <https://doi.org/10.1016/j.precamres.2005.11.002>.
- Zhou, X.Y., Yu, J.H., O'Reilly, S.Y., Griffin, W.L., Sun, T., Wang, X.L., Tran, M.D., and Nguyen, D., 2018b, Component variation in the late Neoproterozoic to Cambrian sedimentary rocks of SW China–NE Vietnam, and its tectonic significance. *Precambrian Research*, v. 308, p. 92–110, <https://doi.org/10.1016/j.precamres.2018.02.003>.
- Zhu, D.C., Zhao, Z.D., Niu, Y.L., Dilek, Y., Wang, L.Q., and Mo, X.X., 2011, Lhasa terrane in Southern Tibet came from Australia. *Geology*, v. 39, no. 8, p. 727–730, <https://doi.org/10.1130/G31895.1>.
- Zhu, G.L., Yu, J.H., Zhou, X.Y., Wang, X.L., and Wang, Y.D., 2019b, The western boundary between the Yangtze and Cathaysia blocks, southwest South China block: Precambrian Research, v. 331, <https://doi.org/10.1016/j.precamres.2019.105350>.
- Zhu, Y., Lai, S.C., Qin, J.F., Zhu, R.Z., Zhang, F.Y., Zhang, Z.Z., and Zhao, S.W., 2019a, Neoproterozoic peraluminous granites in the western margin of the Yangtze block, South China: Implications for the reworking of mature continental crust. *Precambrian Research*, v. 333, <https://doi.org/10.1016/j.precamres.2019.105443>.
- Zou, H., Bagas, L., Li, X.Y., Liu, H., Jiang, X.W., and Li, Y., 2020, Origin and evolution of the Neoproterozoic Dengganping Granitic Complex in the western margin of the Yangtze block, SW China: Implications for breakup of Rodinia Supercontinent. *Lithos*, v. 370–371, p. 1–21, <https://doi.org/10.1016/j.lithos.2020.105602>.

SCIENCE EDITOR: WENJIAO XIAO
ASSOCIATE EDITOR: CHANGQING YIN

MANUSCRIPT RECEIVED 26 NOVEMBER 2021
REVISED MANUSCRIPT RECEIVED 25 JANUARY 2022
MANUSCRIPT ACCEPTED 25 FEBRUARY 2022

Printed in the USA